FINAL REPORT

Investigation of Chemically Vapor Deposited Tantalum for Medium Caliber Gun Barrel Protection

SERDP Project WP-1425

OCTOBER 2008

Prof. Roland A. Levy
New Jersey Institute of Technology

This document has been approved for public release.

DoD EPA DOE SERDP
Strategic Environmental Research and Development Program

This report was prepared under contract to the Department of Defense Strategic Environmental Research and Development Program (SERDP). The publication of this report does not indicate endorsement by the Department of Defense, nor should the contents be construed as reflecting the official policy or position of the Department of Defense. Reference herein to any specific commercial product, process, or service by trade name, trademark, manufacturer, or otherwise, does not necessarily constitute or imply its endorsement, recommendation, or favoring by the Department of Defense.

Table of Contents

List of Acronyms iv
Acknowledgments 1
Executive Summary 2
1.0 Objective 4
2.0 Background 5
2.1 Problem Addressed by This Technology 5
2.2 Chemical Vapor Deposition 6
3.0 Materials and Methods 8
3.1 Materials 8
3.1.1 Substrates 8
3.1.2 Chemical Precursors 9
3.2 Methods 9
3.2.1 Selection of $TaCl_5$ as a precursor for PECVD Ta deposition 9
3.2.2 Description of PECVD reactor 12
3.2.3 Deposition of PECVD Ta Coatings 14
3.2.4 Description of UVCVD Reactor 15
3.2.5 Deposition of UVCVD Ta Coatings 15
3.2.6 Characterization of Ta Coatings 15
4.0 Results and Accomplishments 17
4.1 Results 17
4.1.1 Growth Rate 17
4.1.2 Topographical and Step Coverage Characterization 19
4.1.3 Crystallographic Structure 23
4.1.4 Compositional Analysis 27
4.1.5 NRA Analysis 30
4.2 Accomplishments 32
5.0 Conclusions and Recommendations 33
5.1 Conclusions 33
6.0 Appendices 34
6.1 Technical Publications 34
6.1.1 Technical Paper 34
6.1.2 Technical Reports 34
6.1.3 Conference/Symposium Presentations 34
6.1.4 Published Technical Abstracts 34
6.1.5 Text Books and Book Chapters 34
References 35

List of Figures

Figure 1. Illustration of conformal step coverage of CVD Ta coating [2]. 6
Figure 2. Schematic diagram of CVD process. 7
Figure 3. SEM image of cross section of patterned Si wafer (145 μm depth, 103 μm width, and 70.3° V-groove angle) 8
Figure 4. Vapor pressure of tantalum halide precursors versus temperature [4]. 10
Figure 5. (a) Enthalpy and (b) Gibbs free energy change versus temperature. 11
Figure 6. Schematic diagram of PECVD reactor. 13
Figure 7. Schematic of 100 mm thermocouple wafer. 14
Figure 8. Correlation of measured surface temperatures to setting temperatures. 14
Figure 9. Representative schematic diagram of UVCVD system. 15
Figure 10. Growth rate of CVD Ta coatings versus RF plasma power 17
Figure 11. Growth rate of CVD Ta coating versus sublimator temperature 18
Figure 12. Growth rate of CVD Ta coatings versus substrate temperature 19
Figure 13. SEM surface images and EDX elemental analysis of CVD Ta coatings deposited inside threaded nut 20
Figure 14. SEM surface images of PECVD Ta coatings deposited on polished AISI 4340 steel coupons and seed layers of Nb, Au, and TaN_x (magnification of 100K). 20
Figure 15. SEM images of cross sections of PECVD Ta coatings. 21
Figure 16. AFM topography of CVD Ta coatings deposited on polished steel coupons. 22
Figure 17. SEM (a) surface and (b) cross section images of UVCVD Ta coatings 23
Figure 18. XRD patterns of CVD Ta coatings deposited on polished steel substrates under various deposition conditions. 24
Figure 19. XRD patterns of Ta coatings deposited on electroplated and sputtered Cr inter layers on top of steel coupons 25
Figure 20. XRD patterns of CVD Ta coatings deposited on Nb, and Au inter layers on top of steel coupons 26
Figure 21. Grazaing Incidence-XRD patterns of Ta coating on Au interlayer 26
Figure 22. XRD patterns of Ta coatings deposited on TaN_x inter layers 27
Figure 23. XRD patterns of Ta coatings deposited on steel substrates by UVCVD 28
Figure 24. AES depth profiles of PECVD Ta coatings deposited on polished steel substrates at the RF input power of (a) 60 and (b) 100 W 29
Figure 25. Depth profile of XPS spectra for CVD Ta coatings deposited on polished steel coupons 30
Figure 26. AES depth profiles of UVCVD Ta coating deposited on steel substrates 31
Figure 27. NRA depth profile of hydrogen present in the Ta coated steel 31

List of Tables

Table 1. Properties of tantalum halide precursors [4] 9

List of Acronyms

AES	Auger electron spectroscopy
AFM	Atomic Force Microscopy
AISI	American Iron and Steel Institute
APCVD	Atmospheric pressure chemical vapor deposition
ARL	Army Research Laboratory
at.%	Atomic percentage
Au	Gold
C	Carbon
Cl	Chlorine
Cr	Chromium
Cr (VI)	Hexavalent chromium
CVD	Chemical vapor deposition
DoD	Department of Defense
E_a	Activation Energy
EDX	Energy dispersive X-ray Spectroscopy
°F	Degree(s) Fahrenheit
FE-SEM	Field emission scanning electron microscopy
H	Atomic hydrogen
H_2	Hydrogen gas
He	Helium
hr	Hour(s)
HSS	High-strength steel
I.D.	Inside diameter
IM-CMS	Internally magnetized cylindrical magnetron sputtering
N_2	Nitrogen gas
Nb	Niobium
NJIT	New Jersey Institute of Technology
NH_3	Ammonia gas
NRA	Nuclear reaction analysis
O	Atomic oxygen
O_2	Oxygen gas
O.D.	Outside diameter
OEM	Original equipment manufacturer
OSHA	Occupational Health and Safety Agency
PECVD	Plasma-enhanced chemical vapor deposition
ppm	Part per million
PVD	Physical vapor deposition
Ref.	Reference
RF	Radio frequency
$R_{R.M.S.}$	Root mean square roughness
sccm	Standard cubic centimeter per minute
SEM	Scanning electron microscopy
SERDP	Strategic Environmental Research and Development Program
SiC	Silicon carbide

List of Acronyms (continued)

TACOM	Army Tank Automotive Command (now TACOM Life Cycle Management Command)
Ta	Tantalum
$TaBr_5$	Tantalum Pentabromide
$TaCl_5$	Tantalum Pentachloride
TaF_5	Tantalum Pentafluoride
TaN_x	Tantalum Nitride
UV	Ultra-violet
UVCVD	Ultra-violet Chemical Vapor Deposition
wt.%	Weight percentage
XPS	X-ray Photoelectron Spectroscopy
XRD	X-ray Diffraction
XRR	X-ray Reflectivity

Acknowledgments

This SERDP-sponsored program has been made possible by the technical contributions and numerous valuable suggestions of the team members including Dr. Jeffrey M. Warrender at Benet Laboratories, Dr. Jonathan S. Montgomery at Army Research Laboratory, Mr. Jeffrey Darbig at Picatinny Arsenal, and Dr. Thomas R. Gaffney at Air Products. This program could not possibly have been performed with the diligent work of the NJIT Post-Doc staff, namely Dr. Yong Suh and Dr. Sungmin Maeng who were instrumental in carrying out the synthesis and characterization tasks on the Ta coatings as well as Mr. Weizhong Chen, a former graduate student who participated in all aspects of this program and earned his Ph.D at NJIT as a result. Thanks are due to Mr. H. Tridandam and Mr. K. S. Cuthill at Air Products who helped greatly in carrying out the tantalum deposition experiments. Special thanks are reserved to the Contract Officer Representative John Beatty as well as the Technical Program Managers at SERDP, namely Mr. Charles Pellerin and Mr. Bruce Sartwell who provided continued guidance and generous advice throughout this program.

Executive Summary

The overall objective of this SERDP-supported program (WP-1425) was to investigate the use of chemical vapor deposition (CVD) to produce high quality tantalum (Ta) coatings for wear and erosion protection of medium caliber gun barrels. In addition to offering an environmentally benign alternative to chromium (Cr) plating, this relatively low temperature process proved to provide high throughput, low cost, conformal step coverage, and coatings with desirable properties and performance.

Chromium is widely used as a protective coating on the interior bore surfaces of medium caliber gun barrels to reduce the erosive effects of hot propellant gases and the mechanical effects of the projectiles. Current coatings are electro-deposited from aqueous solutions of hexavalent chromium, a known carcinogen and toxic substance that is strictly regulated and entails high disposal costs. Tantalum has been selected as an attractive candidate for Cr replacement because it is environmentally friendly and exhibits excellent physical and chemical properties such as a high melting point (3017°C), good ductility, and excellent corrosion resistance in aggressive environments. Although internally magnetized cylindrical magnetron sputtering (IM-CMS) has been employed to produce Ta coatings to protect large caliber gun bores, it has proven to be deficient in its performance on cylinders with diameters below 45 mm due to the critical ionization distance required by this process.

In the first year of this program, it was demonstrated that CVD Ta coatings could be successfully synthesized on steel substrates by plasma enhancement using tantalum pentachloride ($TaCl_5$) as a precursor. The Ta coatings were shown to be dense, continuous, and essentially pure. Furthermore, it was shown that CVD Ta coatings can be deposited uniformly and conformally inside cylindrical tubes that replicate the shape of plain and rifled gun barrels. Additionally, evaluation of the environmental impact of the CVD Ta deposition process was successfully completed.

In the second year of this program, the effort focused on synthesizing CVD tantalum coatings on steel substrates to optimize the deposition process with respect to growth rate and alpha phase formation. The interrelationships governing the growth kinetics, compositions, and coating properties were established as a function of deposition temperature, total pressure, reactant concentration, and reactor geometry. In the attempt to insure formation of CVD Ta coatings with the α phase, deposition experiments were conducted using polished AISI 4340 steels with various seed layers including electroplated and sputtered Cr, sputtered Nb, sputtered Au, and non-stoichiometric tantalum nitride (TaN_x). These experiments revealed that in-situ sequential deposition of CVD TaN_x and CVD Ta lead to preferred formation of the alpha phase.

In the third year of this program, the chemical, structural, and morphological properties of the Ta coatings were established. The results indicated that the coatings were essentially pure and dense independent of deposition parameters. The results also indicated that these coatings exhibit a near perfect step coverage and a crystallographic structure that is dependent on pre-treatment procedures. A major shortcoming of the aforementioned process was the low growth rate achieved as a result of the relatively lower temperatures imposed by the experimental constraints of the PECVD deposition apparatus. That constraint was lifted by making use of UV assisted

CVD which proved to produce α-phase Ta coatings with significantly higher growth rates at temperatures higher than those used in PECVD but still within the tempering temperature range of medium caliber gun barrel steel.

1.0 Objective

Chromium is widely used as a protective coating on the interior bore surfaces of medium caliber gun barrels to reduce the erosive effects of hot propellant gases and the mechanical effects of the projectiles. Current coatings are electro-deposited from aqueous solutions of hexavalent chromium, a known carcinogen and toxic substance that is strictly regulated and entails high disposal costs. Although internally magnetized cylindrical magnetron sputtering (IM-CMS) has been demonstrated to be capable of depositing tantalum coatings to protect large caliber gun bores, it has proven not to perform well on cylinders with diameters below 45 mm due to the critical ionization distance required by this process.

In accordance with Executive Order (13148: Part 2), a 50 % reduction was required in the use of hexavalent chromium (primary component of electrodeposition) by December 31, 2006. As a result of this ordinance, several efforts were initiated to investigate the use of environmentally friendly processes to produce Ta as an alternative material to Cr for protection of gun bores from erosion and corrosion.

This program addressed this need by investigating the use of chemical vapor deposition (CVD) to produce high quality tantalum coatings for wear and erosion protection of medium caliber gun barrels. In addition to offering an environmentally benign alternative to chromium plating, this relatively low temperature process promised to provide high throughput, low cost, conformal step coverage, and coatings with desirable properties and performance.

The viability of this CVD tantalum process was to be demonstrated through:

- Investigation of growth rates as a function of processing parameters to ascertain process throughput.
- Evaluation of the effects of surface preparation treatments on coating quality and performance.
- Determination of coating composition as a function of processing parameters to establish achievable degree of chemical purity.
- Characterization of the coatings in terms of their mechanical, structural, and morphological properties to assemble a comprehensive property data base.
- Evaluation of coating performance through a complete series of tests that included adhesion, thermal shock, abrasion, as well as wear, erosion, and corrosion resistance in realistic configurations.
- Assessment of gun bore erosion, firing accuracy, and rifling durability through actual firing studies.
- Analysis of scale-up potential for commercial viability and technology transfer.

2.0 Background

2.1 Problem Addressed by This Technology

Chromium is widely used as a protective coating on the interior bore surfaces of medium caliber gun barrels to reduce the erosive effects of hot propellant gases and the mechanical effects of the projectiles. Current coatings are electro-deposited from aqueous solutions of hexavalent chromium, a known carcinogen and toxic substance that is strictly regulated and entails high disposal costs. In the past, chromium has proven to be quite effective due to its chemical inertness as well as its excellent adherence and close thermal match to the substrate. However, current lethality requirements have increased to the point where chromium has become thermally overmatched and the resulting wear life has declined to unacceptable levels. Furthermore, the cracking tendency of chromium remains a serious issue that is incompatible with the ever-increasing need for higher muzzle energies (~20 MJ) and hotter propellants (~3700 °K). Chromium cracking provides a path for the hot propellant gases to reach the lower melting substrate, resulting in a lift-off of the coating and subsequent exposure of the underlying steel to excessive wear and erosion.

The dual challenge of replacing the toxic chromium plating process and extending the barrel life by introducing a superior wear and erosion material was addressed through the use of internally magnetized cylindrical magnetron sputtering (IM-CMS) of tantalum. The IM-CMS process is preferable to electro-plating for several reasons:

- It is a dry (non-aqueous) environmentally friendly process
- It offers an attractive plug-in solution to the existing gun barrel manufacturing sequence
- The properties of the underlying steel are unaffected by deposition of the sputtered coating
- Acceptable deposition rates can be attained
- Post-processing is unnecessary.

In comparison to Cr, Ta offers advantages that include a higher melting point (3017 °C versus 1857 °C) and higher ductility (in case of α-Ta) that leads to better resistance to thermal shock and cracking and, thus, higher resistance to corrosive propellant by-products attack of the substrate.

Although IM-CMS is an acceptable method for cylinders with internal diameters of 60 mm and greater, it has proven not to perform well on cylinders with diameters below 45 mm since the smaller bore diameter of medium caliber guns cannot accommodate the critical ionization distance required for this process. The fact that sputtering is generally a room temperature process limits inter-diffusion at the substrate-coating interface. This creates adhesion difficulties, which in turn leads to more extensive surface preparation (cleaning). Furthermore, room temperature sputtering of Ta typically favors formation of the undesirable β-phase that is about 5 times harder than the α-phase and, therefore, much less ductile and more susceptible to cracking. Another important consideration particularly pertinent to medium caliber guns, where the bores are rifled as compared to being smooth for large caliber guns, is that sputtering is a “line-of-sight” technique, thus, limiting the uniform coverage required for proper wear and erosion protection along spiraled paths.

Chemical vapor deposition (CVD) offers promising solutions to the problems associated with IM-CMS coatings. Reported studies have demonstrated the use of CVD in producing Ta coatings from tantalum halide sources [1-5]. High quality CVD Ta coatings were produced with excellent step coverage in sub-micron trench structures with high aspect ratios as shown below in Figure 1 [2].

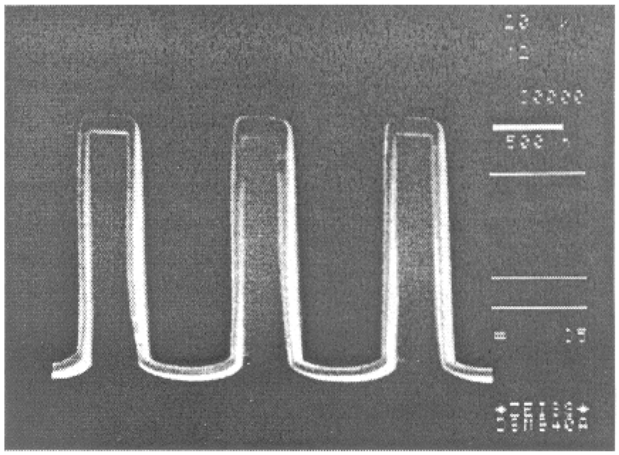

Figure 1. Illustration of conformal step coverage of CVD Ta coating [2].

2.2 Chemical Vapor Deposition

CVD offers a promising alternative to resolve the problems associated with IM-CMS coatings. CVD is a well-established technique that is widely used for a wide range of coating applications. A large variety of materials can be synthesized by CVD. These materials comprise insulators and dielectrics, elemental and compound semiconductors, electrical conductors, and superconductors [6]. In addition to its unique versatility, this material synthesis method can operate at relatively low temperatures (e.g. by using plasma or ultra-violet), thus, reducing the underlying substrate to experience process induced crystallographic changes or damage, and contamination by diffusion of impurities [7].

CVD is defined as a process whereby constituents of the gas or vapor pressure react chemically on a substrate surface to form a solid product (Figure 2). This product can be in the form of a thin film, a thick coating, or even, if allowed to grow further, a massive bulk. Depending on the growth conditions, it can have a single crystal, polycrystalline, or amorphous structure. Typical CVD processes are surface-catalyzed reactions (i.e., heterogeneous as compared to homogeneous where the reactions nucleate in the gas phase). The occurrence of a chemical reaction distinguishes CVD from physical vapor deposition (PVD) processes, such as sputtering and evaporation. Chemical reactions that can take place include pyrolysis (thermal decomposition), oxidation, reduction, hydrolysis, nitride and carbide formation, synthesis reactions, disproportionation, and chemical transport. Deposition variables such as temperature, pressure, input concentrations, gas flow rates, and reactor geometry determine the deposition rate and the deposit properties.

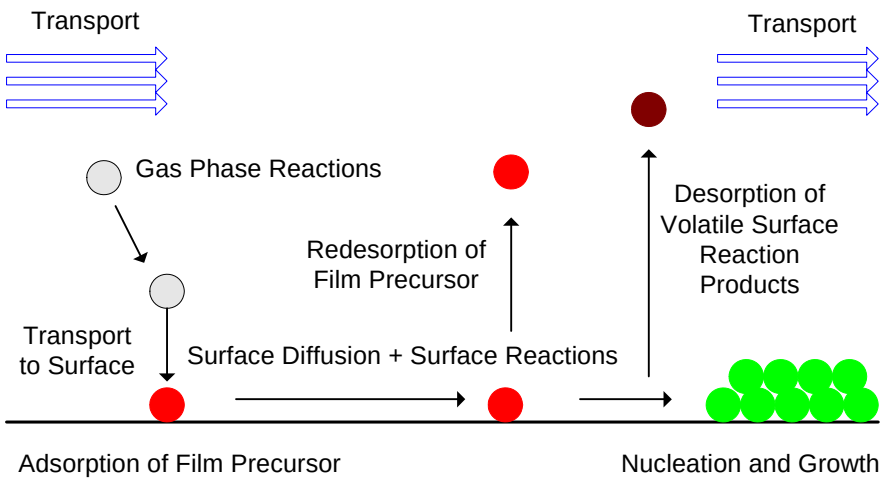

Figure 2. Schematic diagram of CVD process.

CVD processes are classified according to the type of energy supplied to initiate and sustain the reaction: (1) Thermally activated reactions at various pressure ranges, where heat is applied by resistance heating, RF induction heating, or infrared heating. (2) Plasma promoted reactions, where an RF (or DC) induced glow discharge is the source for most of the energy that initiates and enhances the rate of reaction. (3) Photon-induced reactions, where radiation of a given wavelength triggers and sustains the reaction by direct photolysis or by an energy transfer agent, such as ultraviolet-activated mercury.

Optimization of the CVD process has proven to yield coatings that are adherent, highly dense, chemically pure, and uniform in thickness as well as in composition. Optimized process parameters also have resulted in CVD coatings that exhibit low intrinsic stress, desirable microstructures, and a good surface finish. However, the key property that distinguishes CVD from PVD is its superior surface conformability (or surface coverage). The large values of the mean-free path (resulting from the use of high vacuum conditions) and the high sticking coefficient of the atoms render PVD processes largely "line-of-sight" depositions. In CVD, the mean-free path of the molecules and their sticking coefficients are often reduced. This means that the "precursor" undergoes a large number of collisions upon entering the reactor before it collides with a surface. Because of these collisions, the lower sticking coefficients of the molecules (compared to the atoms produced in PVD), and the enhanced surface diffusion caused by the heated substrate, CVD processing often yields perfectly conformal surface coverage. In the microelectronics industry, CVD metal coatings (e.g., Ta, W, Cu, Al, etc.) are routinely used to conformally cover sub-micron-sized trenches (< 0.12 μm) with severe aspect ratios (hole depth/diameter ratio ~ 20:1) [8-15]. This feature uniquely offered by the CVD process is highly beneficial in achieving the required uniform coating coverage along the interior rifled surface of the gun barrel. It is also worthwhile pointing out that the CVD technique is amenable to sequential in-situ deposition of different layers. Such a process would, thus, facilitate the deposition of a thin TaN_x under-layer to improve adhesion of the Ta coating and to enhance formation of the desirable α-Ta phase.

3.0 Materials and Methods

3.1 Materials

3.1.1 Substrates

The substrates used for the CVD Ta deposition consisted mainly of AISI 4340 steel coupons (non-polished and polished) and pieces from plain and patterned silicon wafers. The polished steel coupons were prepared by mechanically polishing them with silicon carbide (SiC) pads followed by diamond suspensions of decreasing particle size down to 0.05 μm. Silicon wafers with V-groove patterns (shown in Figure 3) were used to evaluate the step coverage of CVD Ta coatings. In addition to those steel and silicon wafer substrates, threaded nuts with dimension of 6.4 mm I.D. and 10 mm length were used as substrates to replicate the riffled shape of gun barrels.

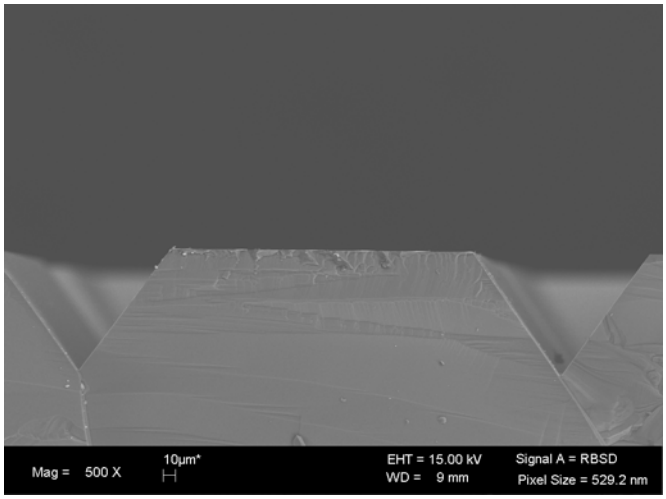

Figure 3. SEM image of cross section of patterned Si wafer (145 μm depth, 103 μm width, and 70.3° V-groove angle)

In an effort to produce CVD Ta coating with the pure α phase, deposition experiments using polished AISI 4340 steel coupons with a Cr interlayer on top were conducted under optimal deposition conditions. The Cr interlayer was formed using both sputtering and electroplating processes. For the sputtered Cr interlayer, the deposition conditions were 300 W plasma power, 7.7 mTorr process pressure, and ~ 200 °C substrate temperature. Electroplated interlayer Cr coatings were also produced at Benet laboratories using a conventional plating process.

In addition to the use of a Cr interlayer, an investigation involving the deposition of other interlayer materials on polished AISI 4340 steel substrates was conducted to establish if such material would enhance formation of the α-phase Ta. These sputtered materials included niobium (Nb) that exhibits very similar lattice parameters to those of alpha Ta and gold (Au) which has the added advantage of not growing an oxide on the surface. These interlayer coatings were produced using a Kurt Lesker sputtering system at an argon (Ar) pressure of 10 mTorr and at a power of 100 – 200 W.

In addition to the use of Nb and Au interlayers, it was discovered that non-stoichiometric $TaN_{0.1}$ can be produced with a perfect match to the α phase of Ta. The use of such an interlayer turned out to be ideal in this case as it can be deposited sequentially and in-situ within the CVD reactor prior to Ta coating deposition. Experiments were thus conducted using in-situ sequential deposition of non-stoichiometric TaN_x interlayer coatings followed by CVD Ta coatings. These CVD TaN_x coatings were synthesized with the use of precursors consisting of either nitrogen (N_2) or ammonia (NH_3) in the presence of tantalum pentachloride ($TaCl_5$).

3.1.2 Chemical Precursors

In this work, tantalum chloride ($TaCl_5$) and tantalum bromide ($TaBr_5$) were used as precursors for the PECVD and UVCVD processes, respectively. Hydrogen (H_2) gas was used in both processes as a reducing agent. Helium (He) was added in the case of the PECVD process to promote the excitation and ionization process [16].

3.2 Methods

3.2.1 Selection of $TaCl_5$ as a precursor for PECVD Ta deposition

In this section, the rationale in selecting $TaCl_5$ as a choice precursor for plasma enhanced CVD Ta deposition is presented. The use of tantalum halide precursors such as TaF_5, $TaCl_5$, and $TaBr_5$ has been reported in the synthesis of CVD Ta coatings. The melting and boiling points of these precursors are found to increase in the following order: $TaF_5 < TaCl_5 < TaBr_5$ (Table 1). At a given temperature, the vapor pressure of these halides consequently follows a reverse order: $TaBr_5 < TaCl_5 < TaF_5$ (Figure 4). At delivery point, higher vapor pressure gases are preferred. The overall chemical reaction involved in CVD Ta using tantalum halides is as follows:

$$TaX_5(g) + 2.5H_2(g) = Ta(s) + 5HX(g), \text{ where X represents F, Cl, or Br} \qquad \text{[Eq. 1]}$$

Table 1. Properties of tantalum halide precursors [4]

Precursors	Melting point (°C)	Boiling point (°C)	Heat of Formation (ΔHf, kcal/mol)
TaF_5	97	230	-455
$TaCl_5$	216	242	-205
$TaBr_5$	265	349	-143

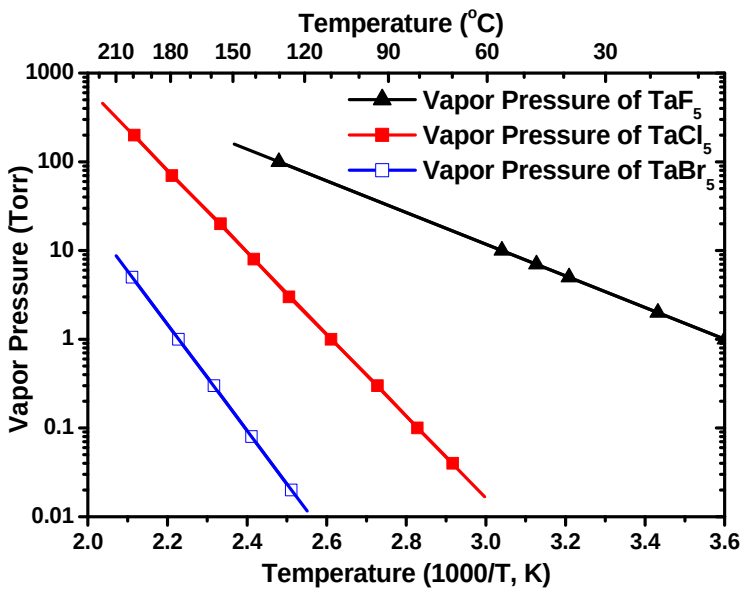

Figure 4. Vapor pressure of tantalum halide precursors versus temperature [4].

Our thermodynamic calculations show that the aforementioned reaction is endothermic (Figure 5a). The enthalpy change for the reaction with TaF_5 is much greater than reactions involving $TaCl_5$ and $TaBr_5$ indicating that a CVD Ta process based on TaF_5 is expected to require more energy than processes based on the other two precursors. Additionally, the Gibbs free energy change indicates that reactions with $TaCl_5$ and $TaBr_5$ show a greater tendency for spontaneity as compared to TaF_5 as the temperature increases (Figure 5b). Based on this data, $TaCl_5$ emerged as a promising precursor candidate for Ta deposition using PECVD. $TaCl_5$ is a white crystalline solid at room temperature with a 1 Torr vapor pressure at ~ 110°C. It has a heat of formation of -205 kcal/mol, bonding energy of ~ 41 kcal/mol, and melting point of 210 °C and can readily be stored in a stainless steel bubbler.

Thermodynamic calculation of the Gibbs free energy change for the above reaction (Eq. 1) reveals that a thermal CVD Ta process requires very high temperature in order for the reaction to become spontaneous (Figure 5b). However, the use of plasma in the CVD Ta process can significantly lower the deposition temperature. In the presence of plasma, $TaCl_5$ and H_2 gas are dissociated into active species according to the following reaction:

$$TaCl_5 + e^- \rightarrow TaCl_{5\text{-}x}(g) + xCl(g) + e^- \qquad \text{[Eq. 2]}$$

and

$$H_2(g) + e^- \leftrightarrow 2H(g) + e^- \qquad \text{[Eq. 3]}$$

Both Eq. 2 and Eq. 3 lead to the following reactions:

$$TaCl_{5\text{-}x} + \frac{(5\text{-}x)}{2}H_2(g) \rightarrow Ta(s) + (5\text{-}x)HCl(g) \qquad \text{[Eq. 4]}$$

and

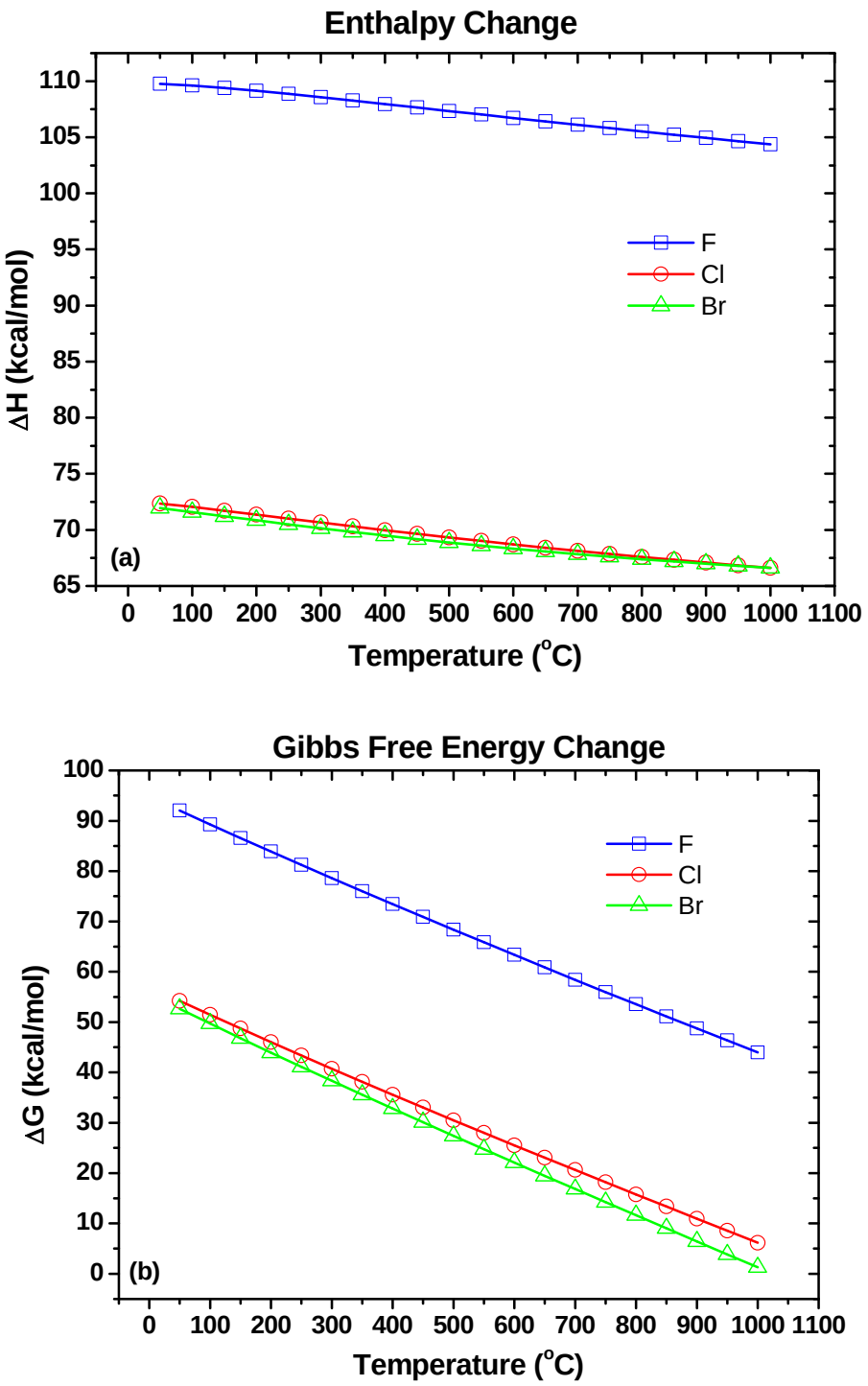

Figure 5. (a) Enthalpy and (b) Gibbs free energy change versus temperature.

$$TaCl_{5-x} + (5-x)H(g) \rightarrow Ta(s) + (5-x)HCl(g) \qquad \text{[Eq. 5]}$$

where x represents the possible integers 1, 2, 3, or 4.

In Eq. 4 and Eq. 5, thermodynamic calculations of the Gibbs free energy change shows that the reaction in the presence of plasma spontaneously occurs even at relatively low deposition temperatures (Figure 5). In the presence of active hydrogen atoms, the reaction spontaneously takes place over the entire temperature regime of interest (Figure 5b).

While the choice of $TaCl_5$ as a precursor in conjunction with the PECVD process was based on its superior vapor pressure to that of $TaBr_5$ which allowed for an easier delivery mechanism of the precursor into the reaction chamber, that choice was not as important when dealing with the UVCVD process where higher deposition temperatures were employed and the ease of dissociation was a better criterion which in turn accounted for the choice of $TaBr_5$ as a precursor in this case.

3.2.2 Description of PECVD reactor

Figure 6 illustrates the schematic diagram of the PECVD reactor used which allowed to process maximum substrates 15 cm in diameter. The reactor was connected to an Edwards QDP 80 vacuum station comprised of a Roots blower and a mechanical pump, which has a pump speed of 375 m^3/h and an ultimate base pressure of 5.3×10^{-3} Torr. The pressure of the reactor was monitored at the reactor inlet using a vacuum gauge with a 0– 10 Torr range and controlled by a throttle valve pressure controller to maintain constant pressure. An Advanced Energy RFX-600 with a frequency of 13.56 MHz was used as the source of radio frequency (RF) power. The power supply was connected to an RF matching network for impedance matching. The reactor was equipped with a load lock to prevent atmospheric contamination. The load lock was isolated from the reactor by a pneumatically operated slit valve and evacuated using a rotary pump. Sample transfer was achieved through a manual load lock arm.

Mass flow controllers (MFC) were used to monitor and control the flow rate of feed gasses. The H_2 reactant gas and the He dilute gas were delivered through a shower head located above the substrate. The shower head also served as the powered RF electrode. The $TaCl_5$ precursor with H_2 carrier gas was delivered through a gas dispersal ring. The cooling ring was attached with the gas dispersal ring to prevent the decomposition of the precursor inside the ring. N_2 was used as a coolant. The precursor was contained in the stainless steel sublimator. The precursor sublimator and delivery line were heated and the temperatures were controlled by a Watlow Anafaze CLS 208 heat controller. The temperature of the delivery line was set higher than that of the sublimator to avoid the condensation of the precursor within the line.

The experiments were conducted with the use of an inorganic scrubber system (Harrington Industrial Plastics' model ECV 56 -5 fume scrubber) connected at the exhaust port of the vacuum pump. In such a scrubber system, all collected gases are circulated within a caustic solution (NaOH) and neutralized at the pH level between 5 and 8. After neutralization, the gases are vented into atmosphere. The scrubber was proven to remove hydrogen chloride and chlorine with 99% yield. Therefore, the chemical species still left in the vented gas consist almost only of

hydrogen and helium as trace diluents in air. Inspection of the Material Safety Data Sheets indicates that neither one of these gases poses a health hazard if properly managed during processing.

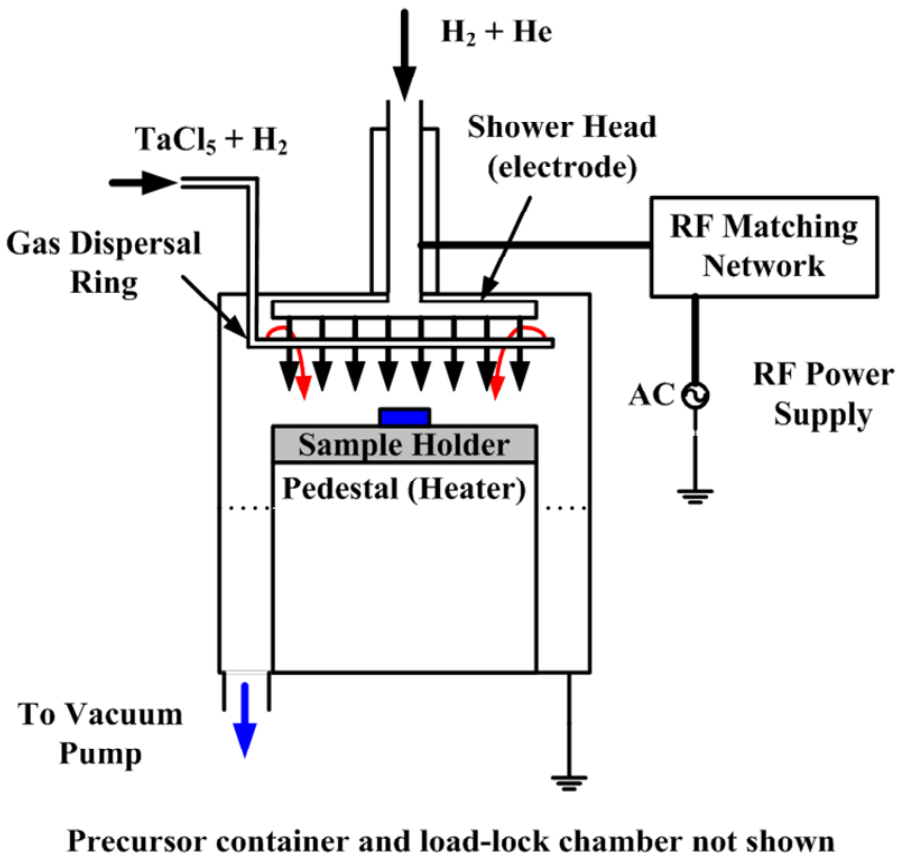

Figure 6. Schematic diagram of PECVD reactor.

The substrates were heated using a resistive heater. The temperature was measured and controlled by a heat controller with a type K thermocouple. The surface temperature of the substrate was observed using a "Thermodynamic Sensors 100 mm thermocouple wafer", as shown in figure 7. Five thermocouples were attached on that wafer. The data was collected through a Pico TC-08 eight channel thermocouple data logger and monitored by a computer. The results are shown in figure 8. The relationship between the temperatures at the surface and the setting point was established by fitting a curve through the following equation (Eq. 6):

$$(\text{Surface Temperature}) = 0.6 \times (\text{Setting Temperature}) + 70 \qquad \text{[Eq. 6]}$$

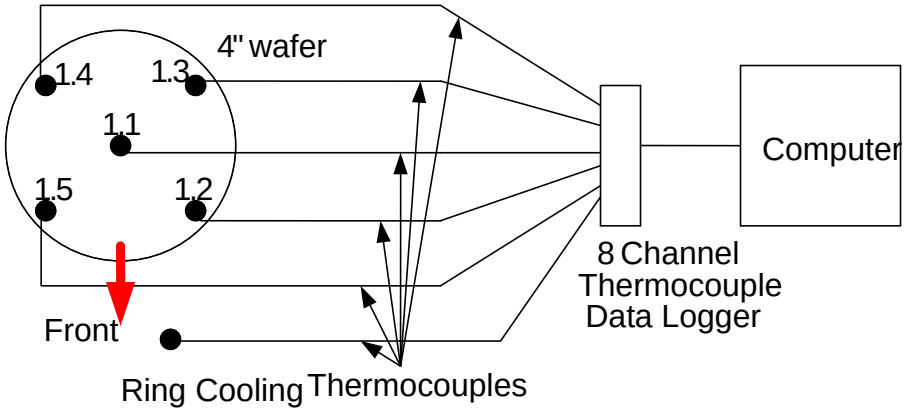

Figure 7. Schematic of 100 mm thermocouple wafer.

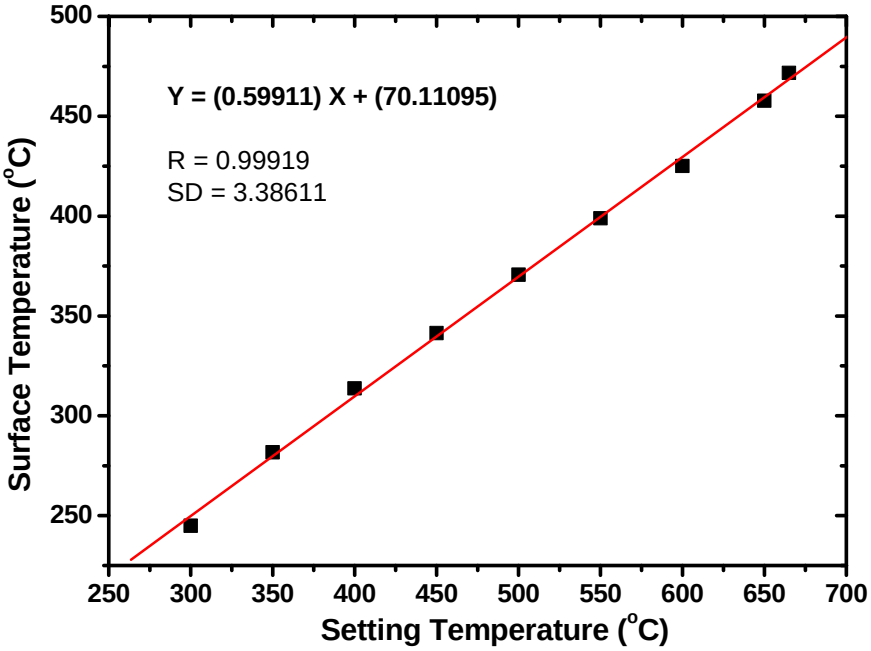

Figure 8. Correlation of measured surface temperatures to setting temperatures.

3.2.3 Deposition of PECVD Ta Coatings

Prior to CVD Ta deposition, the substrates were cleaned in an ultrasonic bath with isopropanol, acetone and methanol sequentially, rinsed with DI water, and dried with clean N_2. After loading the substrates into the reactor, *in-situ* cleaning with active H atoms produced by the RF plasma (100 W) under 5 Torr of H_2 and He at a target deposition temperature for 10 – 20 minutes was conducted to remove native oxide and organic contaminants. The flow rates for H_2 and He gases were 400 and 20 sccm, respectively. The optimization of deposition process, especially for producing Ta coatings with the desirable α-phase was investigated by varying deposition temperature (300 – 460 °C), process pressure (0.7 – 8.0 Torr), RF plasma power (60 – 100 W),

sublimator temperature for precursor (100 – 120 °C), flow rate of H_2 carrier gas (10 – 20 sccm) and distance between the plasma head and substrate (1.5 – 2.5”). In all the Ta deposition experiments, $TaCl_5$ was used as a precursor and H_2 was used as reactant and carrier gas for the precursor. The flow rates of H_2 reactant gas and He gas were maintained at 500 and 20 sccm, respectively. After deposition, the Ta coatings were cooled down to room temperature at N_2 gas environment and rinsed with DI water to remove any left over precursor followed by drying with N_2 gas.

3.2.4 Description of UVCVD Reactor

The ultraviolet chemical vapor deposition (UVCVD) apparatus configuration is similar to that of the PECVD process except for the mode of activating the precursor species. UV lamp operating at a 260 nm wavelength and 100 W were used in this case as the source of excitation. A schematic diagram of the UVCVD system is shown in figure 9.

3.2.5 Deposition of UVCVD Ta Coatings

In the UVCVD experiments, $TaBr_5$ was used as the preferred precursor due to higher operating temperature used in this case and the higher enthalpy of formation associated that molecule and the resulting lower dissociative energy. Such as in the case of PECVD, H_2 was used as a reducing agent. The deposition experiments were conducted at a pressure of 20 Torr, and at deposition temperatures of 600 and 725 °C.

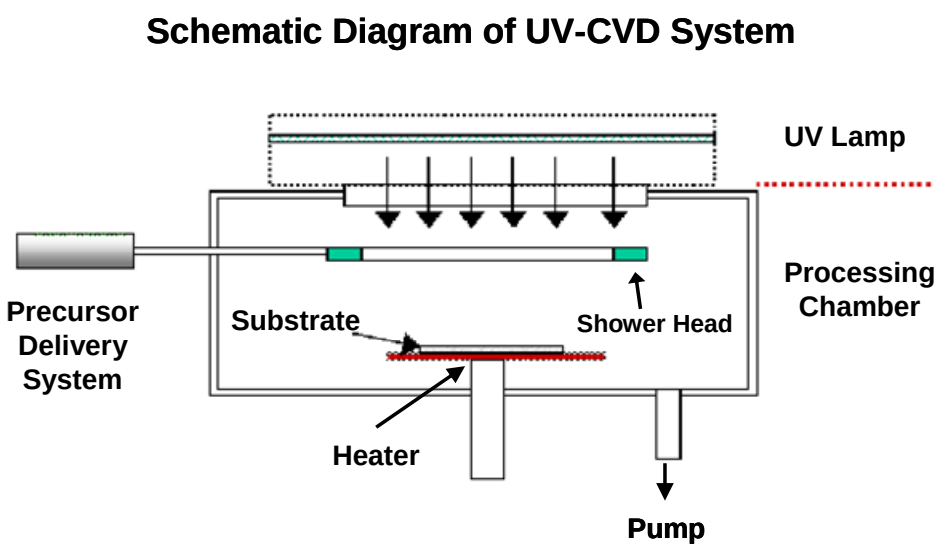

Figure 9. Representative schematic diagram of UVCVD system

3.2.6 Characterization of Ta Coatings

The CVD Ta coatings deposited on steed coupons (AISI 4340) with or without seed layers of Cr, Nb, Au, and TaN_x and Si wafers were characterized in terms of their structural, morphological,

and step coverage properties to assess the viability of the CVD Ta process. Prior to characterization, all the coated samples were ultrasonically cleaned in acetone followed by ethanol. For the cross sectional analysis of the Ta coatings, the specimens were cross-sectioned and mechanically polished using SiC with grit sizes down to 1,200 followed by a polycrystalline diamond suspension with particle sizes down to 0.05 μm.

The surface morphology and conformal coverage of the Ta coatings were investigated using field emission scanning electron microscopy (FE-SEM, LEO 1530 VP) on the surface and cross-sections of coatings deposited on steel coupons as well as Si wafers. A backscattered electron detector was used especially for cross sectional examination of the coatings. Energy dispersive X-ray spectroscopy (EDX, Oxford INCA Energy 400) was carried out for elemental analysis of the coatings. Atomic force microscopy (Nanoscope IIIA Multimode Scanning Probe Microscope) in contact mode was employed to examine the topography and surface roughness of the CVD Ta coatings.

In order to investigate the crystallographic structure of the deposited coatings, X-ray diffraction (XRD) was performed using a Philips X'Pert MRD X-ray diffractometer (Bragg-Brentano θ:θ) with Cu Kα radiation operated at 45 kV and 40 mA. Additionally, grazing Incidence XRD (GI-XRD) with small incidence angle of 0.02° operated 45 kV and 40 mA was performed on the CVD Ta coating deposited on Au seed layer to confirm the presence of α-phase Ta formation.

The compositional analysis was carried out on the CVD Ta coatings using a variety of diagnostic techniques including Auger electron spectroscopy (AES) and X-ray photoelectron spectroscopy (XPS). The operation condition of the AES (Perkin-Elmer Physical Electronic Model 660 Scanning Auger Microprobe) included achieving a base pressure of $< 1.0 \times 10^{-9}$ Torr, utilizing a primary beam energy of 10 keV, and a current of 1.0 μA. To establish a depth profile of the coatings during AES analysis, Ar ion etching was performed with an etching rate of 80 Å/min. In order to evaluate the compositional chemistry of the coatings, XPS (ThermoElectron VG Scientific ThetaProbe) was utilized with an X-ray source of monochromated Al $K\alpha$ (1486.6 eV) operating at 15 kV and 100 W. Survey and profile pass energies used in XPS analysis were 300 and 100 eV, respectively. During the XPS measurements, Ar ion etching was employed for depth profiling with an etching rate of 20 Å/min.

The $^{1}H(^{15}N, \alpha\gamma)^{12}C$ resonance nuclear reaction (NRA) method was employed to verify whether or not hydrogen was incorporated in the underlying substrate during deposition. The Ta coated steel coupon was loaded in the analysis chamber at room temperature and bombarded with ~20 nA of ^{15}N ion. The ion beam energies used for the depth profiles were varied from 6.5 (surface) to 8.0 (base substrate) MeV. By measuring the number of characteristic gamma-ray from this reaction *vs*. beam energy, the H concentration *vs*. depth in the coating sample was established.

4.0 Results and Accomplishments

4.1 Results

4.1.1 Growth Rate

PECVD Ta Coatings

In an effort to optimize the deposition process for producing high quality Ta coatings, the growth rate dependence on plasma power was extensively investigated. In this study, the deposition condition variables were as follows: flow rate of H_2 reactant gas (500 sccm), flow rate of H_2 carrier gas (10 – 20 sccm), total pressure (0.7 – 1.5 Torr), distance between plasma head and substrate (1.5 – 2.5”), deposition temperature (300 – 460 °C), and sublimator temperature for $TaCl_5$ precursor (100 – 120 °C). The nominal RF input power varied from 60 to 100 W. The growth rates of CVD Ta coatings are plotted as a function of actual RF input power in Figure 10. Here, the actual RF input power was obtained by subtracting reflected power from the nominal power. A look at the growth rate data indicates that optimum conditions leading to a growth rate of ~60 Å/min are achieved for a RF power of 65 W at a deposition temperature of 370°C, plasma head to substrate distance of 2”, and sublimator temperature of 110°C. This data indicates that at higher sublimator temperatures and lower plasma head positions contribute to an increased growth rate.

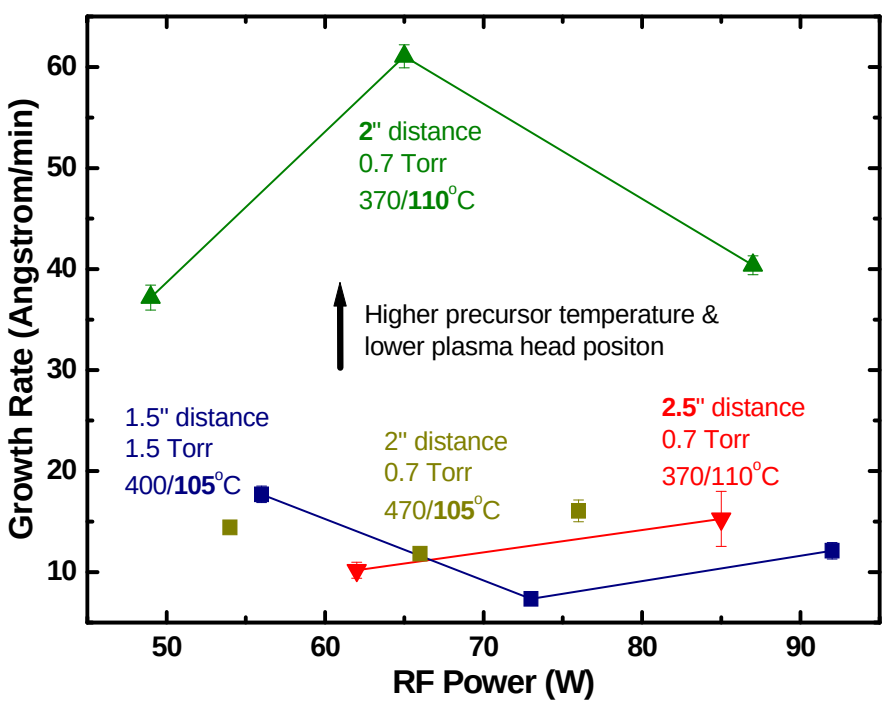

Figure 10. Growth rate of CVD Ta coatings versus RF plasma power

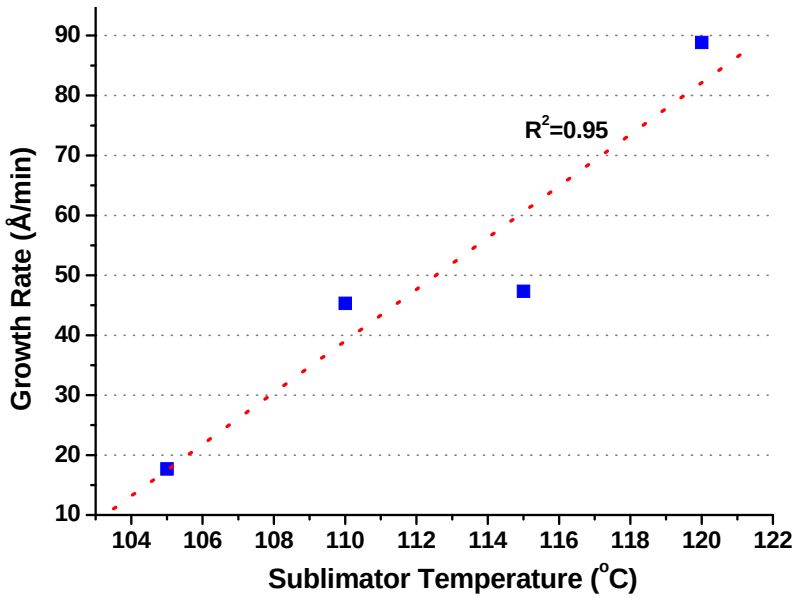

Figure 11. Growth rate of CVD Ta coating versus sublimator temperature

Figure 11 shows the dependence of growth rate on sublimator temperature for a H_2 reactant gas flow rate of 500 sccm, H_2 carrier gas flow rate (10 – 20 sccm), process pressure (1.5 – 2.0 Torr), distance between plasma head and substrate (1.5”), and deposition temperature (400 – 460°C). As indicated in figure 11, the growth rate increases with an increase in sublimator temperatures. When the sublimator temperature is increased, the vapor pressure is also increased thus contributing to the higher growth rate.

The growth rate dependence on substrate temperature is shown in figure 12 at the following deposition conditions: flow rate of H_2 reactant gas (500 sccm), flow rate of H_2 carrier gas (10 sccm), process pressure (2.0 Torr), distance between plasma head and substrate (1.5”), RF power (60 W), and sublimator temperature (120°C). The growth rate is seen here to increase with higher deposition temperature as expected by the Arrhenius relationship. From the slope of this linear dependence, the calculated activation energy was found to be ~ 0.26 eV (~ 25.13 kJ/mol).

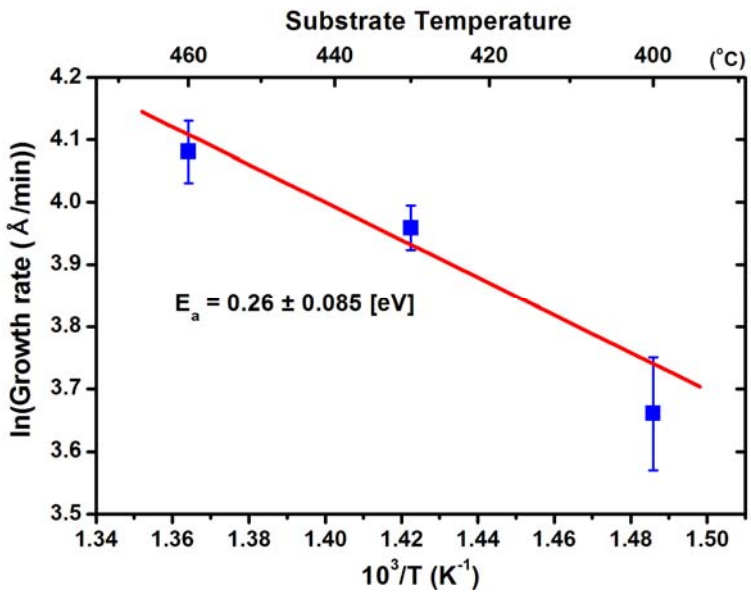

Figure 12. Growth rate of CVD Ta coatings versus substrate temperature

UVCVD Ta Coatings

To increase growth rate of the Ta deposits, it was deemed essential to increase deposition temperature. However, in view of the limitations associated with the PECVD apparatus, an alternative approach was required which led to the investigation of the UVCVD process. As previously mentioned, $TaBr_5$ and H_2 were chosen for this reduction reaction process. Experiments were conducted at a pressure of 20 Torr and at deposition temperatures of 600 and 725°C. At 600°C, the observed growth rate was ~700Å/min while at 725°C, a growth rate of ~ 1000 Å/min was achieved. It is worth noting that a temperature of 600°C is still within the tempering temperature range of medium caliber gun barrel steel.

4.1.2 Topographical and Step Coverage Characterization

PECVD Ta Coatings

Figures 13 illustrate the morphology of the surface of a CVD Ta coated nut (threaded inside) with the result of elemental analysis by EDX. The results reveal that the overall surface of the substrates is homogeneously covered by the coating. The EDX results indicated that that tantalum is the dominant specie.

Figures 14 illustrate the morphology of the surface of CVD Ta coating deposited on polished steel substrate and Nb, Au, and TaN_x seed layers on the top of polished steel substrates. The results reveal that the overall surface of the substrates is homogeneously covered by the coating. The grain size visually evaluated by SEM analysis appears to be on the nano scale (<100 nm).

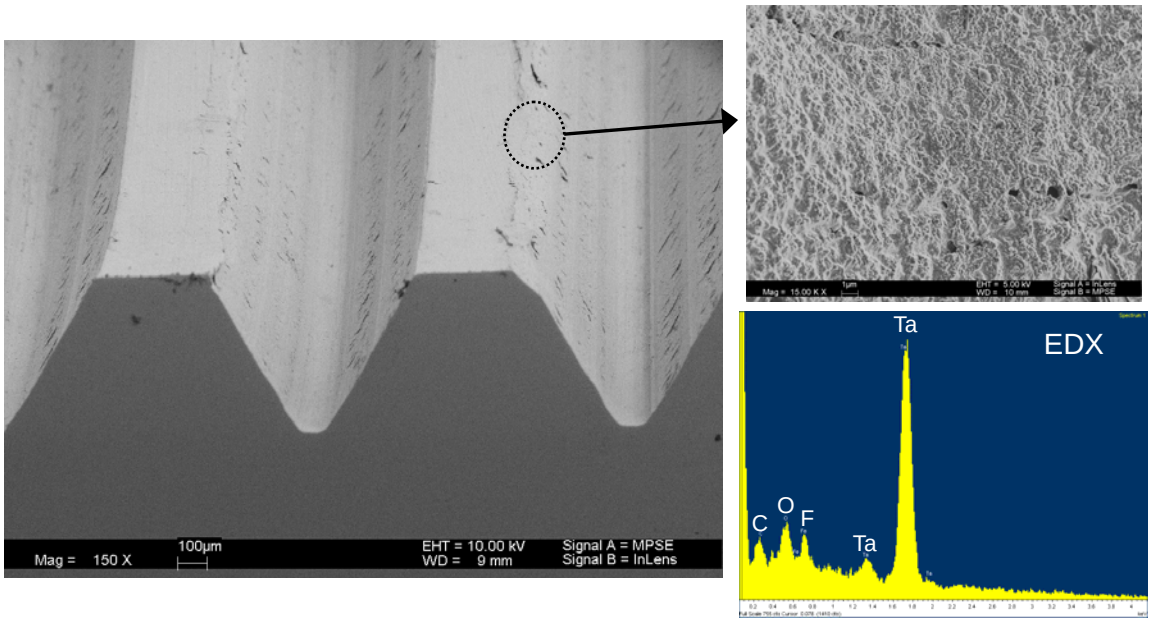

Figure 13. SEM surface images and EDX elemental analysis of CVD Ta coatings deposited inside threaded nut

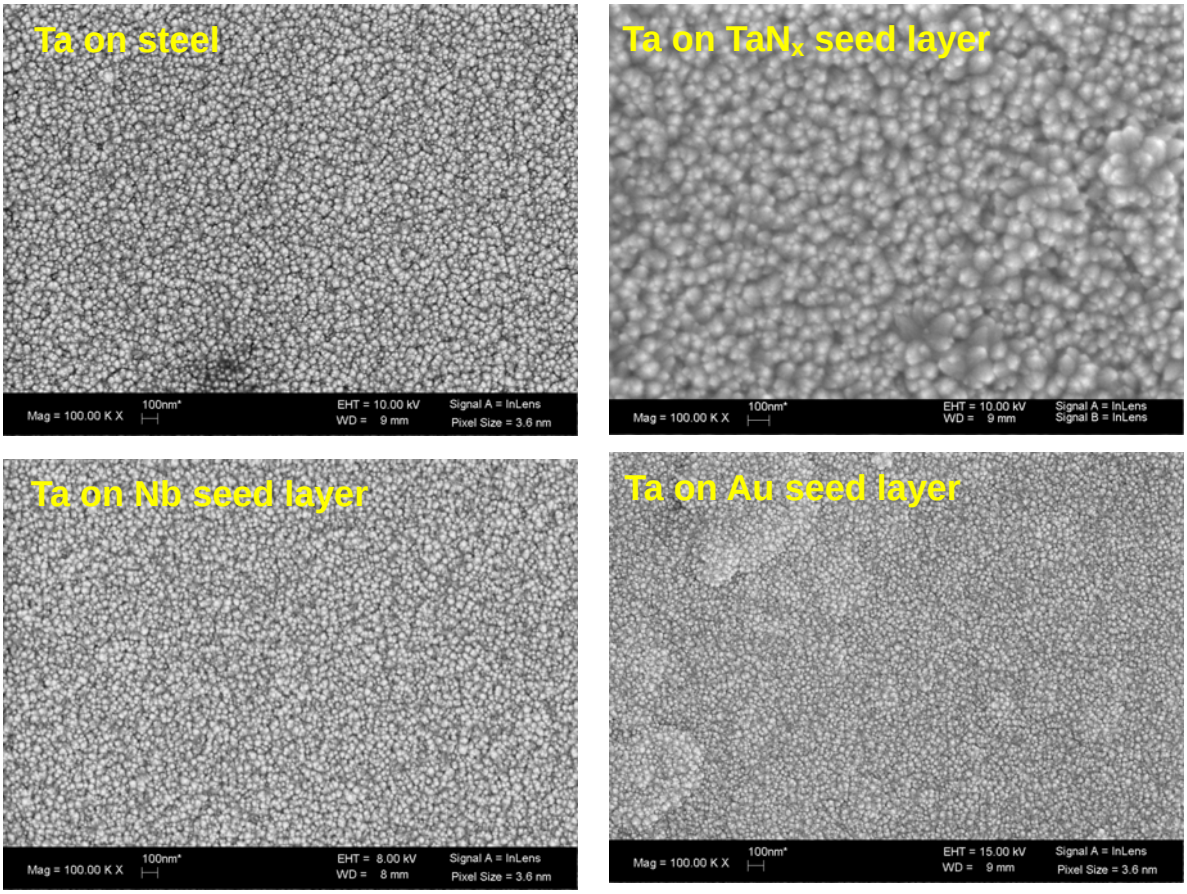

Figure 14. SEM surface images of PECVD Ta coatings deposited on polished AISI 4340 steel coupons and seed layers of Nb, Au, and TaN_x (magnification of 100K)

Cross sectional SEM analysis was conducted to evaluate the conformal coverage of CVD Ta coatings. Figure 15 shows the cross sectional SEM images of the Ta coatings deposited on Si wafer with V-grooves and on polished steel substrates with or without TaN_x seed layer. The results of Ta coatings on the V-grooved Si wafer indicate that the step coverage varied from ~90 % down to ~ 60 % as a function of depth from the surface. In addition, the Ta coatings deposited on the Nb, Au, and TaN_x seed layers exhibit a uniform coating thickness.

Figure 16 illustrates a typical topography observed for Ta coatings deposited on polished steel substrates with different coating thickness. The results indicate that the surface roughness of the Ta coatings increases with increase in coating thickness and exhibit a relatively rougher surface to that of the underlying steel substrate (R_{RMS}=2.84 nm).

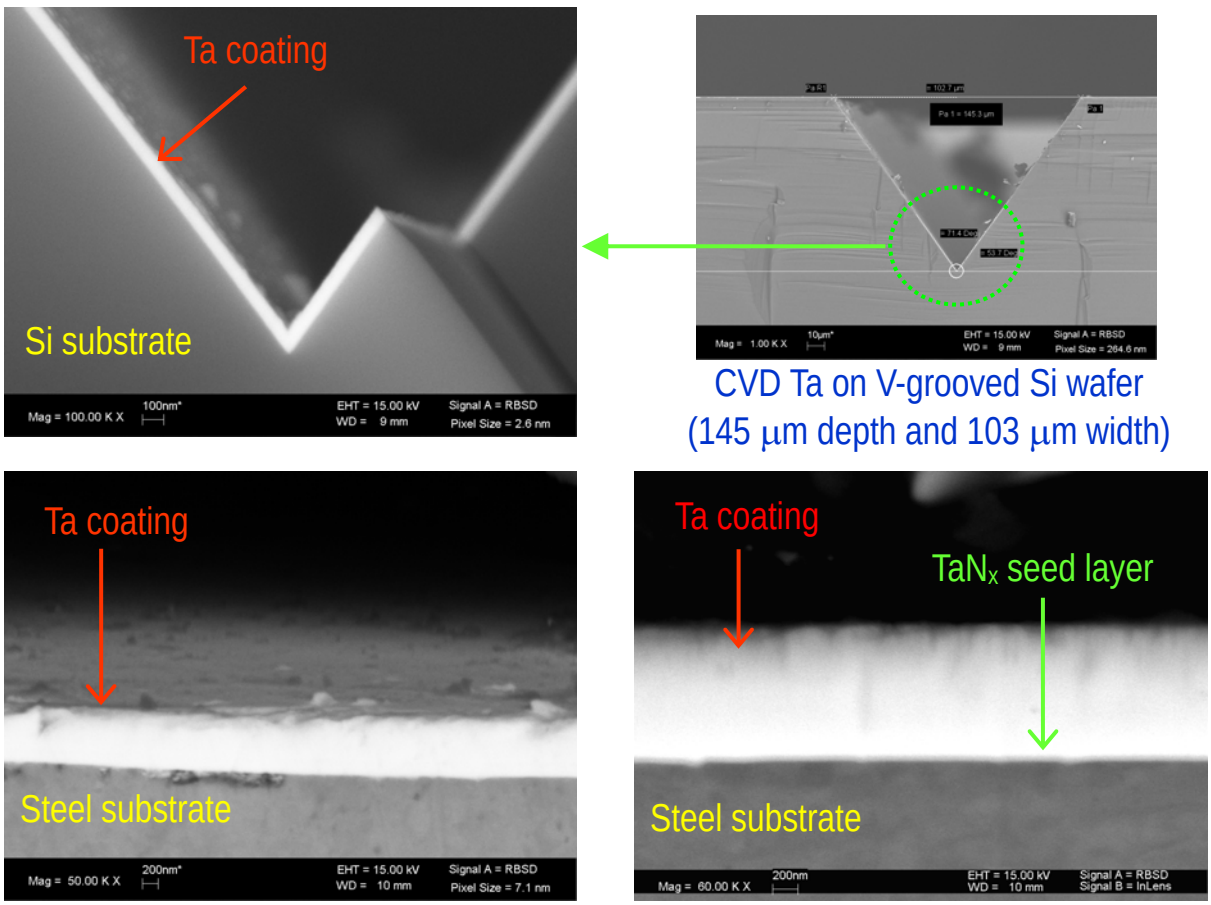

Figure 15. SEM images of cross sections of PECVD Ta coatings.

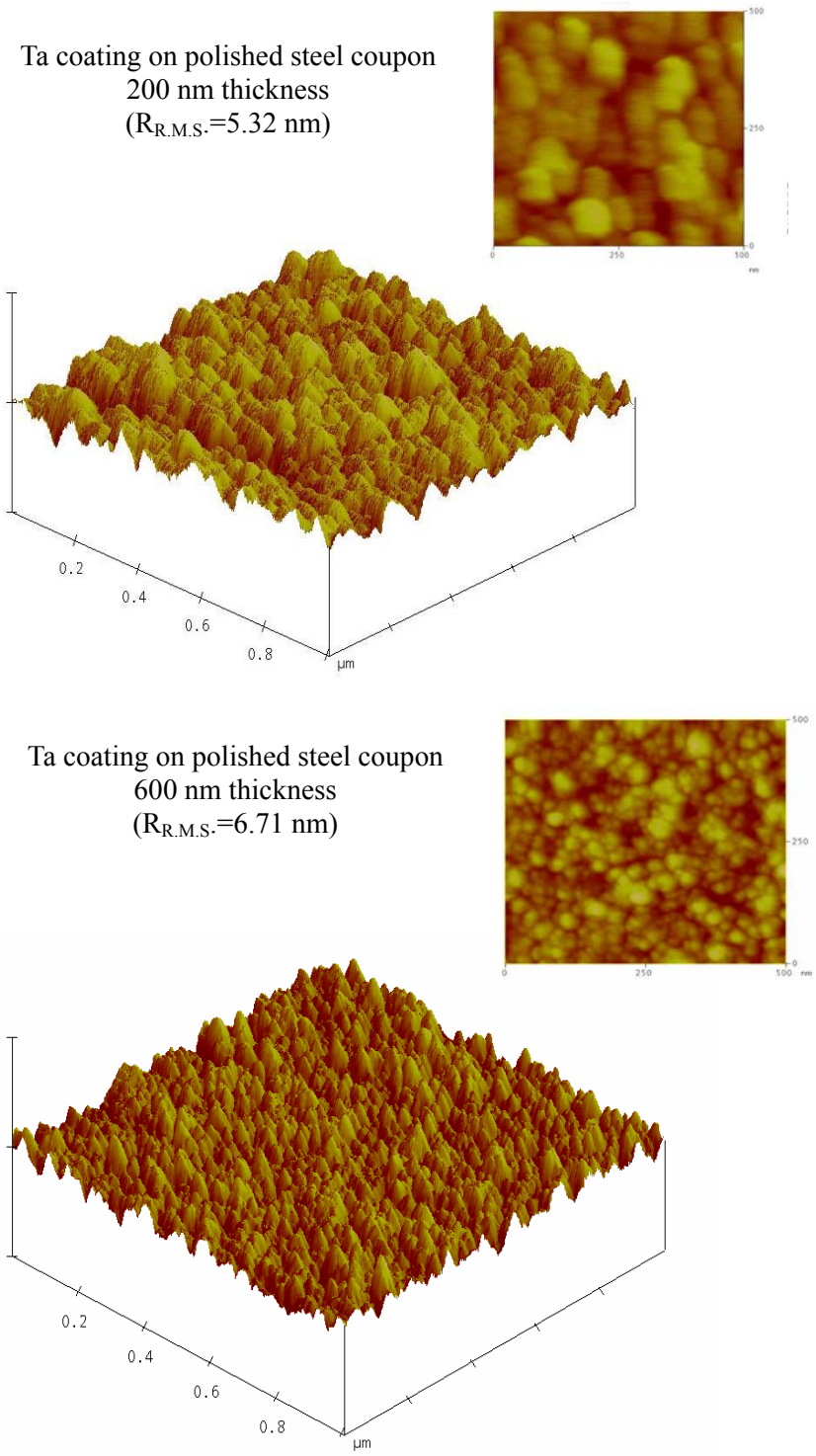

Figure 16. AFM topography of CVD Ta coatings deposited on polished steel coupons.

UVCVD Ta Coatings

Figure 17 represents surface and cross sectional SEM images of Ta coatings deposited on steel substrates by the UVCVD Ta process. The surface morphological analysis reveals that the Ta coatings are dense with relatively larger grains than those of the PECVD Ta coatings. The results of cross sectional analysis demonstrate that UVCVD Ta coatings are also as uniform and conformal as those of PECVD coatings

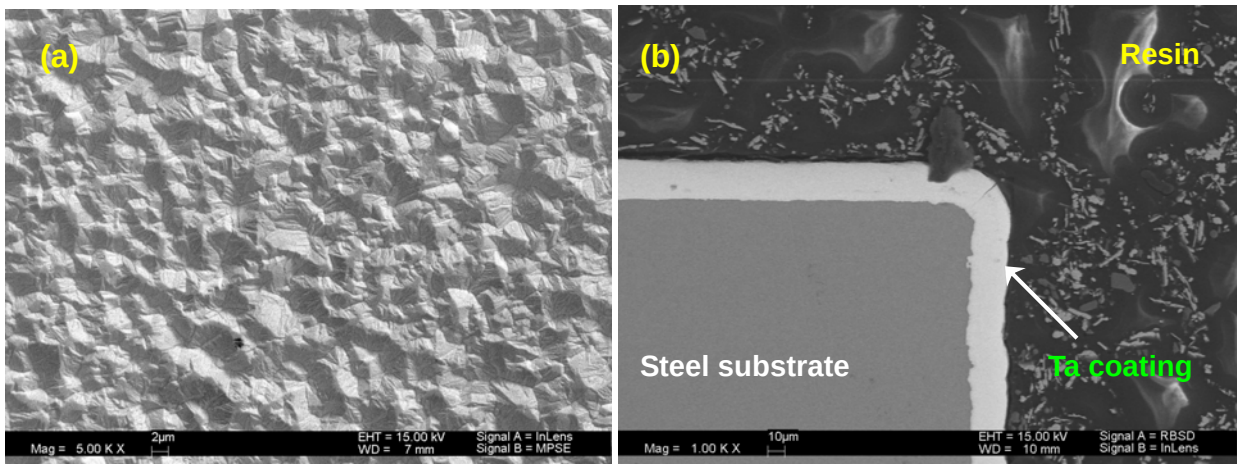

Figure 17. SEM (a) surface and (b) cross section images of UVCVD Ta coatings

4.1.3 Crystallographic Structure

PECVD Ta Coatings

The crystallographic structural study of CVD Ta coatings was conducted using XRD at 45 kV and 40 mA at a two theta (2θ) range of 20 to 140°. In this study, the effect of deposition conditions was investigated. Additionally, the structure of Ta coatings deposited on various interlayers such as Cr (electroplated and sputtered), Nb (sputtered), Au (sputtered), and TaN_x (in-situ CVD) was examined.

Figure 18 shows the XRD spectra of the Ta coatings deposited on steel coupons under various deposition conditions including RF plasma power and distance between plasma head and substrate. The XRD patterns of Ta coatings were compared to those of Ta references consisting of α (body centered cubic structure) and β (tetragonal structure) phases of Ta. The XRD peaks observed at 2θ from 33 – 44° and at ~71°indicate Ta and all other peaks represent those from the underlying steel substrate. At the distance of 1.5” between plasma head and substrate, the Ta coatings exhibit a mixture of α and β-phases with the predominant presence of the β-phase at 33 and 71°. Such a mixture of phases has been encountered in physical vapor deposition (PVD) depending on deposition conditions [17, 18]. At this 1.5” distance, there appears to be no or little effect of plasma power on the phase formation in Ta coatings. At 2.0” distance, Ta coating with RF plasma power of 80 W exhibits a peak with very low intensity at ~33°, representing

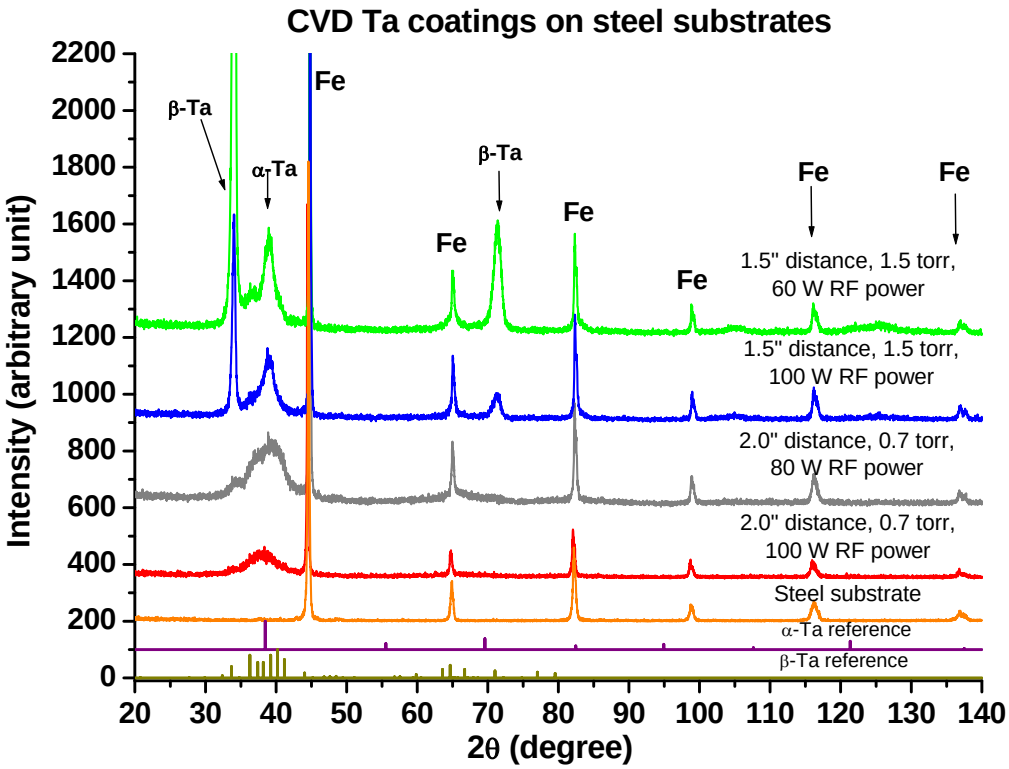

Figure 18. XRD patterns of CVD Ta coatings deposited on polished steel substrates under various deposition conditions.

possibly the presence of β-phase with relatively small portion over α-phase, while such a presence of β-phase in Ta coating with 100 W was identified in the XRD spectra. The broadening of peaks indicating Ta in both of the coatings was observed probably due to either the presence of small grains in nanoscale or amorphous-like structure. Overall, the crystallographic structure of CVD Ta coatings deposited on steel coupons appears to be independent on deposition conditions.

In an attempt to duplicate the Benet Laboratories deposition process which has proven to promote α-phase in Ta coatings produced by IM-CMS, Cr as a seed layer was electroplated on polished steel coupons at their facility. In addition, sputtered Cr coatings were deposited at NJIT for comparative purposes. CVD Ta coatings were subsequently deposited on both of those Cr seed layers with 80 W RF plasma power at 2.0" distance between plasma head and substrate. The XRD spectra of the Ta coatings are shown in Figure 19, compared to those of uncoated Cr seed layers. The peaks at 2θ from 33 to 44° and at 71° indicate Ta and all other peaks represent underlying Cr. The XRD results indicate still the presence of a mixture of α and β phases in these coatings. The discrepancy between this result and those of Benet Laboratories may either be due to a difference in the energetics of the deposited Ta adatoms between PVD and CVD or stem from the pre-deposition steps that are specifically applicable to the PVD coating process but not adaptable to the CVD process.

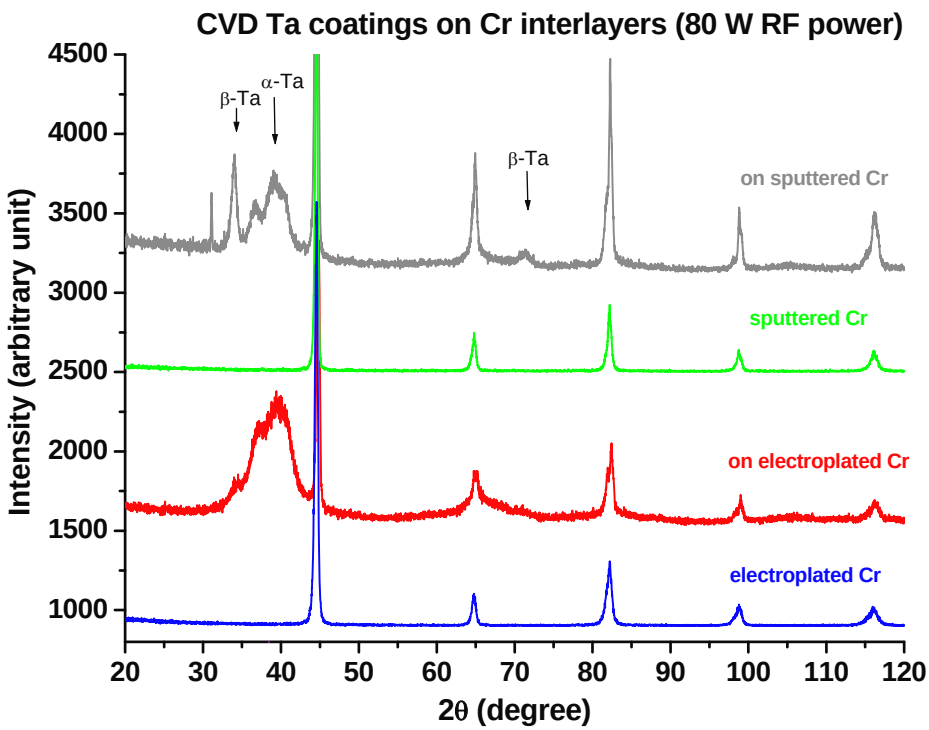

Figure 19. XRD patterns of Ta coatings deposited on electroplated and sputtered Cr seed layers on top of steel coupons

In order to avoid the use of Cr coating as a seed layer and maintain an overall environmentally friendly process, an alternative approach that aims at promoting the α phase formation through the use of an underlying lattice-matched seed layer such as Nb and Au was made. The seed layers of Nb and Au were deposited on steel coupons by PVD (sputtering) and then CVD Ta coatings were deposited on the seed layers. Figure 20 shows the XRD spectra of the Ta coatings compared to those of Ta with α and β phases, Nb, and Au powder references. The XRD results indicate that the Ta coatings no longer reveal evidence of β phase formation. However, no clear presence of α phase could be identified due to peak overlap with that of the underlying seed layers. To resolve this peak overlap observed in conventional XRD, grazing incidence XRD was carried out for the Ta coating on Au seed layer. The grazing incident angle of 0.02° was used so that XRD spectra as shown in Figure 21 were collected only from the Ta coating layer. A peak with low intensity is seen at around 38°, pointing to the presence of α-phase Ta.

In addition to those Nb and Au interlayers, the use of non-stoichiometric $TaN_{0.1}$ as an interlayer with a good lattice match with the α phase of Ta was investigated. Prior to Ta coating deposition, the TaN_x seed layers were deposited on steel coupons sequentially and within the CVD reactor using NH_3 or N_2 in combination with the $TaCl_5$ precursor. A series of deposition experiments to optimize process conditions for producing the desired $TaN_{0.1}$ seed layer were undertaken. XRD results of Ta coatings deposited on TaN_x seed layers revealed a predominant presence of the α phase in the coatings, which render such an approach as quite promising (Figure 22).

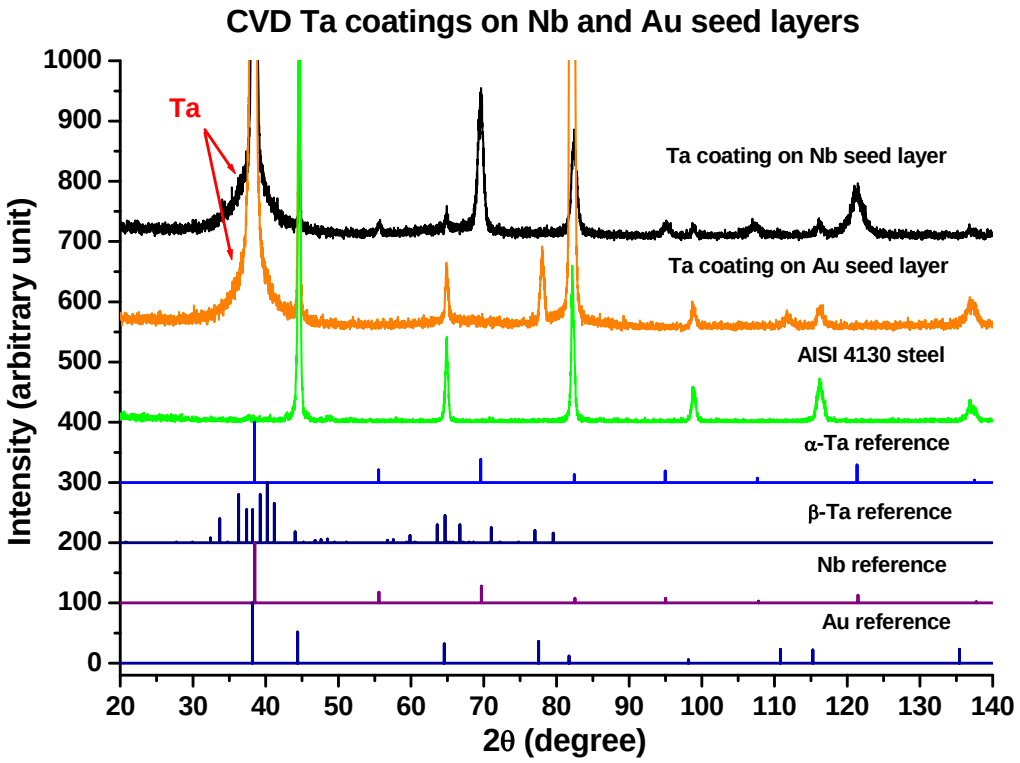

Figure 20. XRD patterns of CVD Ta coatings deposited on Nb, and Au seed layers on top of steel coupons

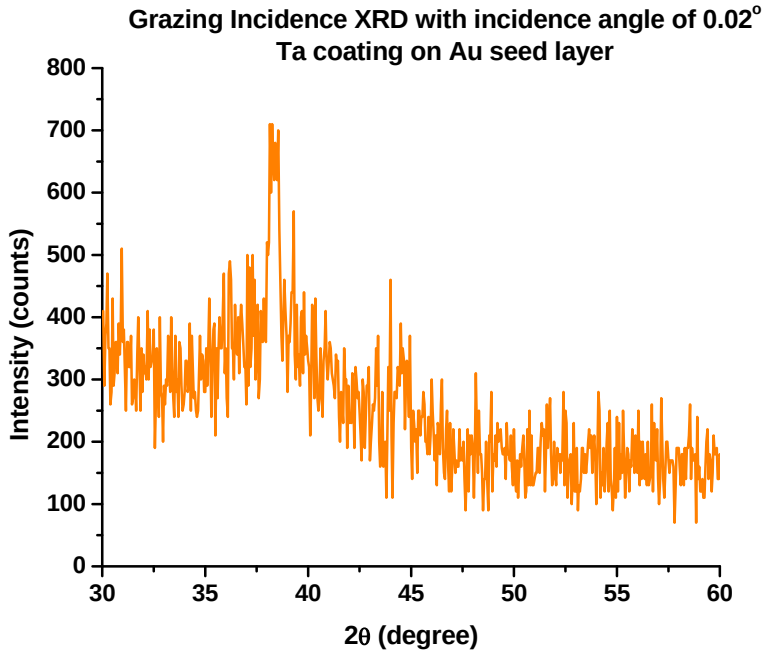

Figure 21. Grazing Incidence-XRD patterns of Ta coating on Au seed layer

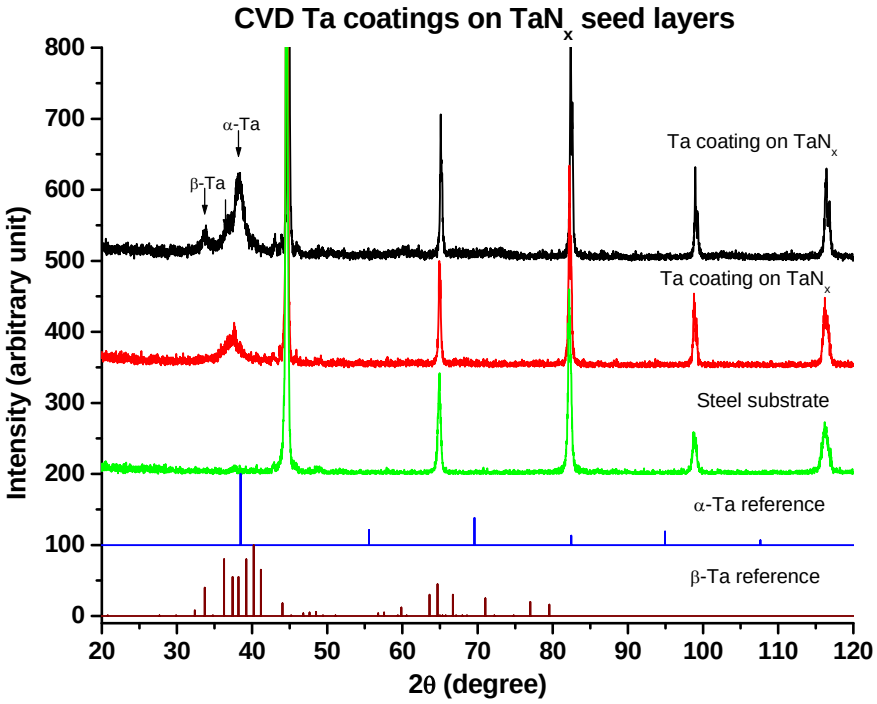

Figure 22. XRD patterns of Ta coatings deposited on TaN_x seed layers

UVCVD Ta Coatings

Figure 23 shows the XRD spectra of the Ta coatings deposited on the steel coupons by UVCVD process with deposition temperatures of 600 and 725 °C using $TaBr_5$ as a precursor. The XRD patterns of Ta coatings were compared to those of Ta references consisting of α (body centered cubic structure) and β (tetragonal structure) phases of Ta. The unmarked peaks in the XRD spectrum for the UVCVD Ta coating at 600 °C represent the presence of the underlying steel substrate and tantalum carbide formed as a result of carbon present as a contaminant at the start of deposition. The Ta coatings deposited at 600 °C exhibit mainly α-phase Ta with a small amount of β phase, while those deposited at higher deposition temperature exhibit only α phase Ta. Overall, the XRD results show that the UVCVD process at such deposition temperatures readily produces the α phase.

4.1.4 Compositional Analysis

PECVD Ta Coatings

To obtain comprehensive information on coating composition as a function of depth, AES analysis was performed on CVD Ta coatings deposited on polished steel coupons under various deposition conditions. AES depth profiles of Ta coatings produced at the RF plasma power of 60 and 100 W are shown in Figure 24. The data reveals that carbon and oxygen are present as impurities on the surface. The chlorine, whose peak is obscured by the low-energy tantalum lines around 160 eV, was found to be present within the detection limit (<1 at.%) of the instrument. Therefore, no depth profile was carried out for chlorine.

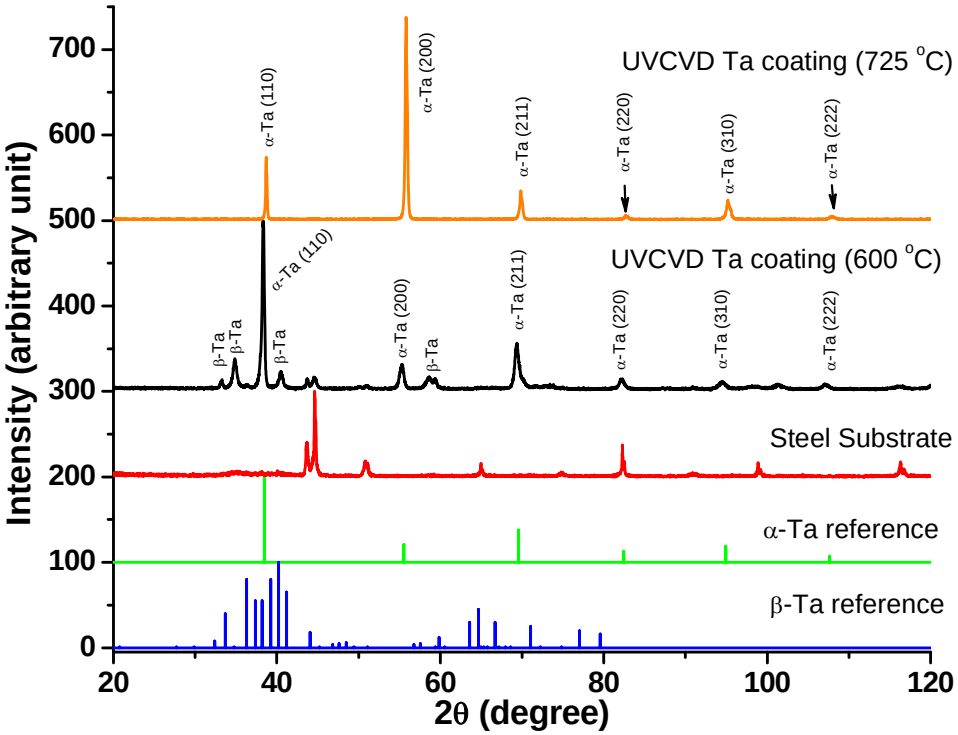

Figure 23. XRD patterns of Ta coatings deposited on steel substrates by UVCVD

The results indicate that the atomic concentration of Ta increases with depth from the surface. The oxygen concentration in the bulk region of the Ta coating with the RF input power of 60 and 100 W was found to be 1.4 and 1.7 at.%, respectively: the carbon concentration for 60 and 100 W was found to be 2.0 and 4.1 at.%, respectively. The presence of oxygen appears to be due to the native tantalum oxide film that naturally forms on the surface. Carbon detected on the surface was removed after the first Ar etching cycle, indicating that the presence of carbon is most likely due to surface contamination. Therefore, the deposition condition appears not to significantly influence the purity of Ta coatings.

In addition to AES depth profile, XPS depth profiling analysis was conducted to obtain the information of composition chemistry of the CVD Ta coatings. The survey spectra of XPS measurements on the coating before depth profiling indicated the presence of oxygen, carbon, and tantalum, which are consistent with the AES results. Figure 25 illustrates typical high-resolution XPS spectra of Ta4f, O1s, and C1s as a function of Ar etching time.

The depth profile of the Ta4f spectra shows multiple peaks indicative of Ta in the oxide form at the surface followed by formation of metallic Ta below the surface (Figure 25). The oxygen peak remains fixed in position of binding energy as a function of depth indicating the presence of a unique tantalum oxide layer (Figure 25). Using the half-maximum intensity of the oxygen signal as the interface marker in the XPS depth profile, the tantalum oxide on the surface was found to be 30~40 Å thick implying the formation of a native oxide film after deposition. Overall, the compositional profile analysis confirmed that the CVD Ta coatings exhibit high purity with minor constituents of oxygen and chlorine in the bulk region.

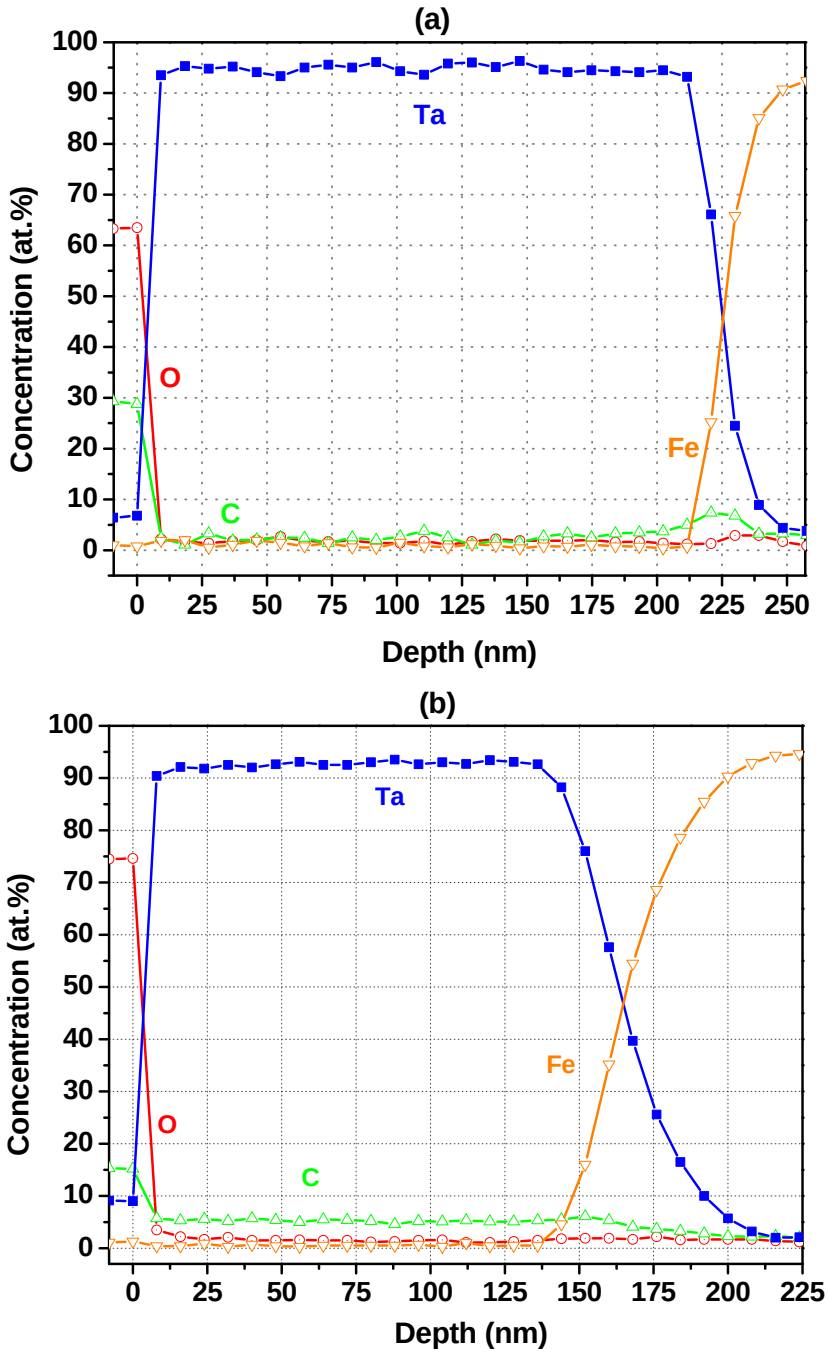

Figure 24. AES depth profiles of PECVD Ta coatings deposited on polished steel substrates at the RF input power of (a) 60 and (b) 100 W

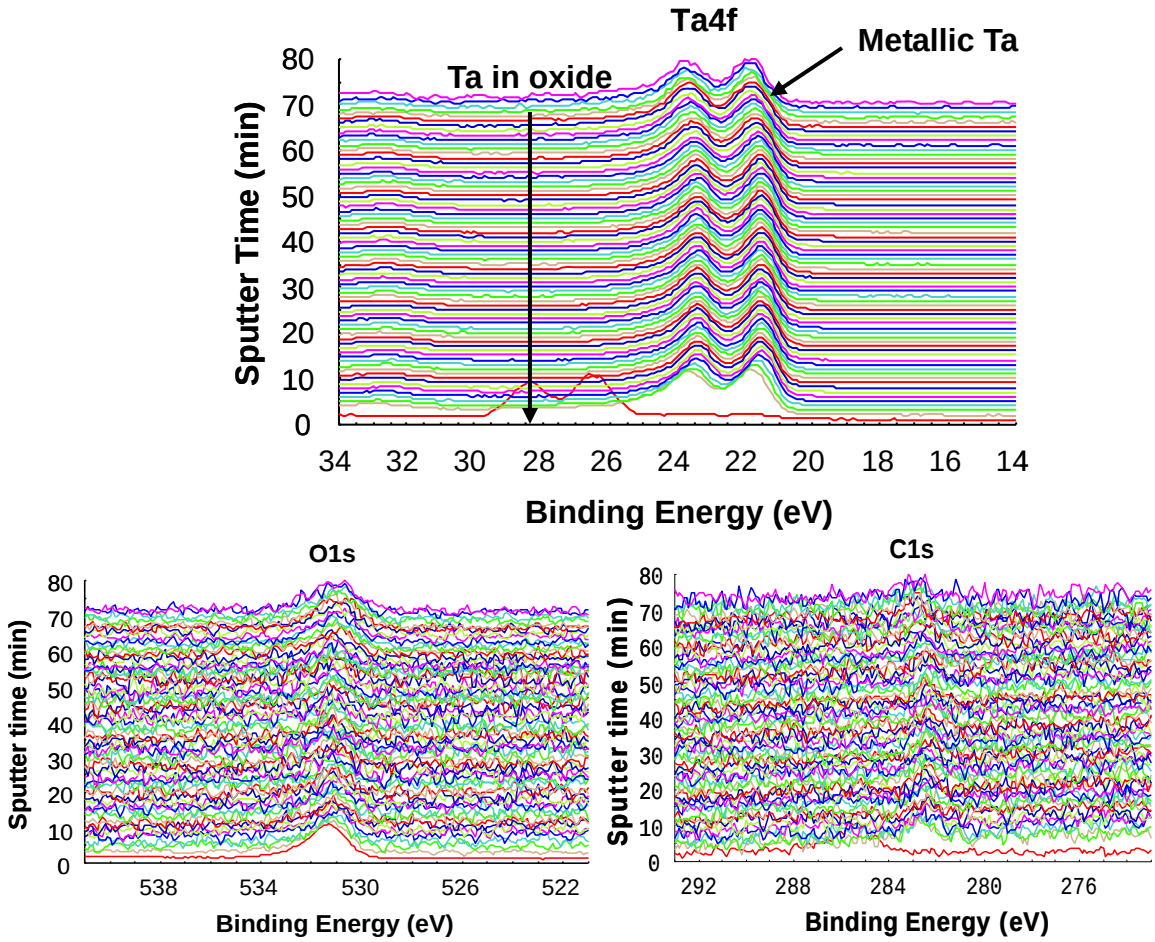

Figure 25. Depth profile of XPS spectra for CVD Ta coatings deposited on polished steel coupons

UVCVD Ta Coatings

Figure 26 shows the result of AES depth profiling on UVCVD Ta coating. The AES analysis reveals high purity Ta coatings with O and C as impurities in bulk region. The presence of oxygen is close to detectable level in the coating and interface, while carbon is present in high concentration at the interface, indicating the contamination of the steel substrate due to the use of a graphite sample holder.

4.1.5 NRA Analysis

Figure 27 shows the concentrations of hydrogen incorporated in the Ta coating and its steel substrate (AISI 4340) versus the coating depth. The results indicate the substrate s contain a H concentration of 24 ppm in weight basis, suggesting that CVD Ta coatings would probably require to undergo a baking treatment to relieve H from the steel substrate as is currently the case for the Cr plating process.

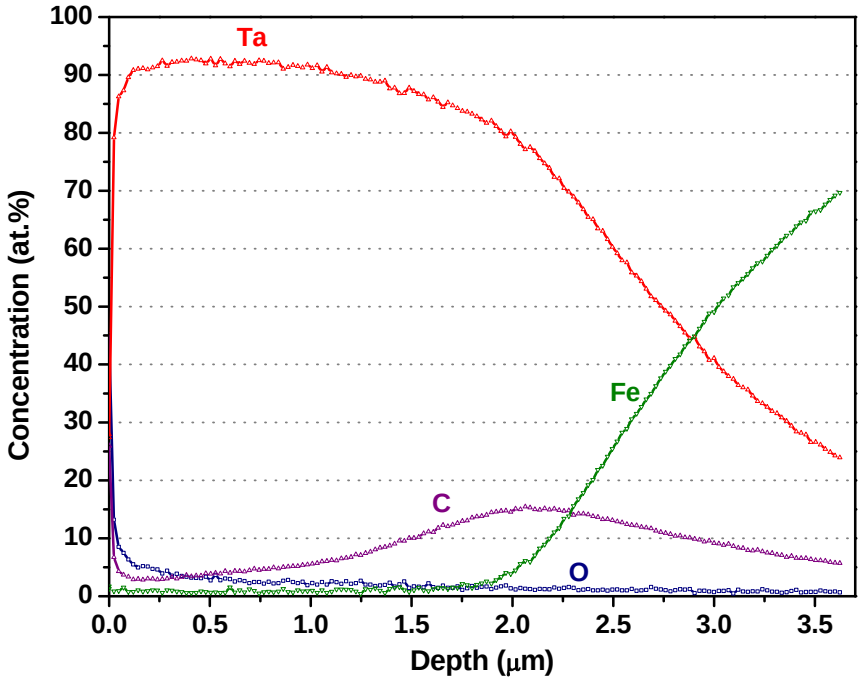

Figure 26. AES depth profiles of UVCVD Ta coating deposited on steel substrates

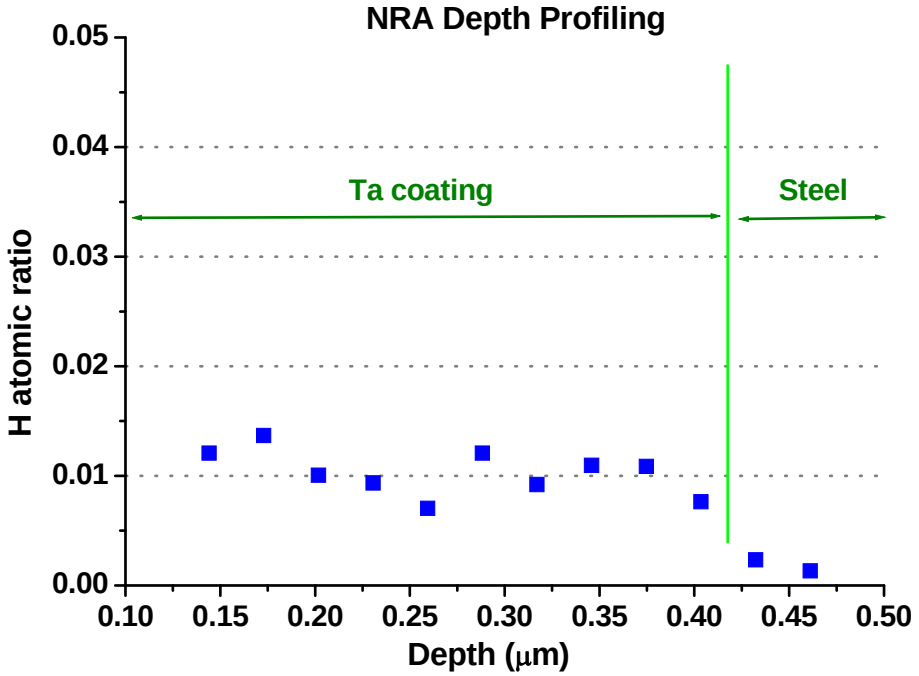

Figure 27. Depth profile of hydrogen present in the Ta coated steel

4.2 Accomplishments

This effort has yielded the following accomplishments in accordance with the proposed tasks:

- Task 1 - Deposition of CVD Ta Coatings

  - Optimized deposition conditions with respect to preferred phase formation of Ta coating and growth rate
  - Investigated effect of processing conditions and various seed layers on Ta phase formation
  - Developed methodology of producing *in-sit*u TaNx seed layer for favoring α phase formation
  - UVCVD was investigated as an alternate process in order to achieve higher growth rates and secure formation of the α phase
    - Preliminary experiments indicate indeed an order of magnitude improvement in growth rate (~1000Å/min)

- Task 2 – Characterization of CVD Ta Coatings

  - Demonstrated through SEM analysis that the Ta coatings exhibit continuous coverage with uniform thickness regardless of deposition conditions and the type of interlayer used
  - Performed compositional analysis (AES and XPS) on Ta coatings. Results confirmed formation of high purity Ta coatings
  - Conducted NRA for H incorporation. Results revealed trace of H incorporation in the underlying base steel
  - Carried out structural studies (XRD) on Ta coatings produced under various deposition conditions with different interlayers and results showed:
    - a mixture of α and β phases in the Ta coatings with Cr seed layers
    - no longer evidence of β phase formation in the presence of Nb or Au interlayers
    - a predominant presence of α phase in the Ta coatings with TaNx seed layers
  - Results of the UVCVD Ta process indicate preferred formation of the desirable α-phase

5.0 Conclusions and Recommendations

5.1 Conclusions

The achieved goals of this program are summarized as follows:

- ✓ Evaluated growth rate dependency on various deposition parameters
- ✓ Investigated effect of processing conditions and various seed layers on Ta phase formation
- ✓ Developed methodology of producing *in-sit*u TaNx seed layer for favoring α-phase formation
- ✓ Demonstrated through SEM analysis that the Ta coatings exhibit continuous coverage with uniform thickness regardless of deposition conditions and the type of seed layers.
- ✓ Carried out structural studies (XRD) on Ta coatings produced under various deposition conditions with different seed layers and results showed:
    - a mixture of α- and β-phases in the Ta coatings with Cr seed layers
    - no longer an evidence of β-phase formation with Nb & Au seed layers
    - predominant presence of α-phase in Ta film with TaNx seed layers
- ✓ Performed compositional analysis on coatings (AES, XPS). Results confirmed formation of high purity Ta coatings under various deposition conditions
- ✓ Investigated UVCVD Ta process which proved to yield order of magnitude higher growth rates than the PECVD process.
- ✓ Characterized UVCVD Ta coatings which were shown to exhibit predominantly a high purity α phase.

6.0 Appendices

6.1 Technical Publications

The following is a list of technical presentations and publications prepared as part of the outreach and communication efforts considered to be an important aspect of sharing information on an important topic and soliciting feedback and comments.

6.1.1 Technical Paper

Y. Suh, W. Chen, S. Maeng, R. A. Levy, "Investigation of Plasma Enhanced Chemically Vapor Deposited Tantalum on High Strength Steels", Material Science & Technology Conference, Detroit, MI (16-20 September, 2007)

6.1.2 Technical Reports

No technical reports, including SERDP Annual Reports, were prepared for external distribution

6.1.3 Conference/Symposium Presentations

Y. Suh, W. Chen, S. Maeng, R. A. Levy, "Investigation of Plasma Enhanced Chemically Vapor Deposited Tantalum on High Strength Steels", Material Science & Technology Conference, Detroit, MI (16-20 September, 2007)

6.1.4 Published Technical Abstracts

1. R. A. Levy, et al. "Investigation of Chemically Vapor Deposited Tantalum for Medium Caliber Gun Barrel Protection", poster presentation at the partners in Environmental Technology Technical Symposium & Workshop, Washington, D.C. (28-30 November, 2006).
2. R. A. Levy, et al. "Investigation of Chemically Vapor Deposited Tantalum for Medium Caliber Gun Barrel Protection", poster presentation at the partners in Environmental Technology Technical Symposium & Workshop, Washington, D.C. (4-6 December, 2007).

6.1.5 Text Books and Book Chapters

No text books, nor chapters, sections, or addenda to books, were prepared for publication.

References

[1] B. C. Arkles and A. E. Kaloyeros, Tantalum and Tantalum-Based Films and Methods of Making the Same", U.S. Patent # 5,919,531, 1999.

[2] X. Chen, H. L. Frisch, A. E. Kaloyeros, and B. Arkles, "Low Temperature Plasma-Promoted Chemical Vapor Deposition of Tantalum from Tantalum Pentabromide for Copper Metallization", J. Vac. Sci. Technol. **B 16**, 2887 (1998).

[3] A. E. Kaloyeros, X. Chen, S. Lane, H. Frisch, and B. Arkles, "Tantalum Diffusion Barrier Grown by Inorganic Plasma-Promoted Chemical Vapor deposition: Performance in Copper Metallization", J. Mater. Res. **15**, 2800 (2000).

[4] T. Kodas and M. Hampden-Smith, The Chemistry of Metal CVD, VCH Publishers Inc., New York, 1994, p. 388.

[5] R. A. Levy, X. Lin, J. M. Grow, H. J. Boeglin, and R. Shalvoy, "Low Pressure Chemical Vapor Deposition of Silicon Nitride Using the Environmentally Friendly Tris(dimethylamino)silane Precursor", J. Mater. Res. **11**, 1483 (1996).

[6] K. L. Choy, "Chemical Vapor Deposition of Coatings", Prog. Mater. Sci. **48**, 57 (2003).

[7] "Microelectronic Materials and Processes", Ed. by R. A. Levy, Kluwer Academic Publishers, Boston, Massachusetts (1989).

[8] N. Ramanuja, R. A. Levy, S. N. Dharmadhikari, E. Ramos, C. W. Pearce, S. C. Menasian, P. C. Schamberger, and C. C. Collins, "Synthesis and Characterization of Low Pressure Chemically Vapor Deposited Titanium Nitride Films Using $TiCl_4$ and NH_3, Mater. Lett. **57,** 261 (2002).

[9] R. A. Levy, M. L. Green, P. K. Gallagher, and Y. S. Ali, "Selective LPCVD Tungsten for Contact Barrier Applications", J. Electrochem. Soc. **133**, 1905 (1986).

[10] M. L. Green and R. A. Levy, "Structure of Selective Low Pressure Chemically Vapor Deposited Films of Tungsten", J. Electrochem. Soc. **132**, 1243 (1985).

[11] L. Green and R. A. Levy, "Chemical Vapor Deposition of Metals for Integrated Circuit Applications", J. Metals **37**, 63 (1985).

[12] M. L. Green, R. A. Levy, R. G. Nuzzo, and E. Coleman, "Aluminum Films Prepared by Metal-Organic Low Pressure Chemical Vapor Deposition", Thin Solid Films **114**, 367 (1984).

[13] R. A. Levy and M. L. Green, "Low Pressure Chemical Vapor Deposition of Tunsten and Aluminum for VLSI Applications", J. Electrochem. Soc. **134**, 37C (1987).

[14] R. A. Levy, M. L. Green, and P. K. Gallagher, "Characterization of LPCVD Aluminum for VLSI Processing", J. Electrochem. Soc. **131**, 2175 (1984).

[15] R. A. Levy, P. K. Gallagher, et al., "Properties of LPCVD Aluminum Films Produced by Disproportionation of Aluminum Monochloride", J. Electrochem. Soc. **132**, 457 (1985).

[16] "Thin Film Processes II", Ed. by J. L. Vossen and W. Kern, Academic Press, Inc., Boston, Massachusetts (1991).

[17] W. D. Westwood, F. C. Livermore, *Thin Solid Films* **5**, 407 (1970)

[18] L. G. Feinstein, R. D. Hutteman, *Thin Solid Film*s **16**, 129 (1973)